A Robust Self-Optimization Algorithm Based on Idiosyncratic Adaptation of Handover Parameters for Mobility Management in LTE-A Heterogeneous Networks

TAREK AL ACHHAB[1], FARIZ ABBOUD[1], AND ABDULKARIM ASSALEM[2]
[1]Department of Communication, Damascus University, Damascus, Syria
[2]Department of Communication, Al-Baath University, Homs, Syria

Corresponding author: Tarek AL Achhab (tarek.alachhab@gmail.com)

ABSTRACT Mobility robustness optimization (MRO) is a fundamental issue regarding self-optimization network (SON). In long-term evolution-advanced (LTE-A), handover (HO) optimization in heterogeneous networks (HetNets) is an urgent need to improve system performance. This improvement is in terms of immunity against unnecessary HO (UHO) such as ping-pong HO (PPHO) and against failed HOs in the sense of radio link failure (RLF) such as too-early HO (TEHO) and too-late HO (TLHO), that is, RLF HO. The occurrence of these undesired HOs increases the consumption of network resources and decreases the quality of service (QoS). In this study, we propose a robust algorithm to reduce the number of PPHO, TLHO, and TEHO events to a minimum by an innovative mechanism that adaptively sets the HO control parameters (HCPs). This reduction is obtained without the need for unjustified techniques that assume certain thresholds for the ratio of PPHOs or the ratio of RLF HOs relative to the total number of HOs, as proposed in the most recent literature. We also present the importance of thinking about the existence of a direct relationship between the hysteresis margin (HM) and time-to-trigger (TTT). We invest this relationship in determining adaptive HCPs. Simulation results show that RLF HOs and PPHOs are minimal, almost zero, compared to the literature and the classical method. This study opens a new avenue for research on mobility management. It reorients research axes toward thinking about the possibility of a correlation between HM and TTT. This is what the research community has not yet realized.

I. INTRODUCTION

Since the first mobile phone was manufactured by Motorola in 1973, mobile phones have become an indispensable technology in our daily lives. Nowadays, the use of mobile phones is no longer limited to providing voice calling services and sending text messages. The functional diversification of this technology includes various data services such as the Internet of Things, mobile games, and live video broadcasting. In this context, mobile data traffic has grown significantly over the past decade; for example, in 2016, it became 18 times what it was in 2011 [1]. In late 2021, it is expected to grow several

times compared to 2016, which represents an increase of approximately 128-fold in only 10 years.

Consequently, many studies are being conducted with the aim of improving the ability of future networks to handle the increasing volume of traffic. For this goal, one could find the reason behind the successive upgradation of wireless communication networks, starting from the first generation (1G), passing through LTE-A. In LTE-A HetNets, the intensive use of small cells, such as microcells, picocells, and femtocells, has become necessary to meet the traffic requirements and to relieve pressure on the macro cells [2]. In fact, the use of small cells resolves the conflict between limited radio resources and data traffic requirements [3]. Moreover, both the network capacity and user QoS are enhanced by small cell

The associate editor coordinating the review of this manuscript and approving it for publication was Cong Pu.

diffusion, although the low-power small cells overlap with the high-power macro cells. This represents a multi-tier network structure known as HetNet.

In parallel, mobility management is becoming more complex because of the significant increase in the size and complexity of HetNets. This was a major reason for developing the concept of SON that has gained increasing importance to achieve the goal of automating the management process and reducing manual intervention [4]. In this context, MRO was introduced as a one-use case of SON. The MRO algorithms refer to procedures that automate the setting of HCPs aimed at minimizing both RLF HO and PPHO events [5], [6].

Hence, HO is a key procedure for mobility management ensuring that users move freely through the LTE-A HetNets while still being connected with the same QoS. In fact, the HO success rate is one of the key indicators of user satisfaction; thus, it is vital that the HO procedure occurs as quickly and as seamlessly as possible [7]. However, the performance and requirements of the HO events of individual users may differ depending on the user's mobility state, such as location and velocity, among other context variables. Therefore, when available, mobility and context information can be exploited to design user-specific and more effective SON algorithms. This is the scope of this paper, where an individualistic adaptive HPC SON algorithm for HetNets is proposed to reduce both RLF HOs and PPHOs. Although the traditional HO mechanism can be described by a very precise flow of events and one can argue that there is little if anything to be improved, the HCP optimization for SON represents one of the most important areas to be researched regarding MRO. Furthermore, it is considered a nascent field of research. This field does not look at modifying the HO flow, but rather at making the HCP settings sufficiently flexible by adjusting them accordingly. The main challenges facing such an MRO algorithm for SON are to find a perfect balance between HM and TTT values, and simultaneously ensuring that the network is in a stable operating point for a long time with as few RLF HOs and PPHOs as possible. Introducing the overlaid HetNets implies that the function of HO should evolve from two points of view: first, maintaining connectivity and second enhancing the entire network's performance. Furthermore, owing to the small coverage and low transmission power of small cells, the HO procedure is much more complicated and needs to be more intelligent. This paper focuses on the optimization of the system-level HCPs in the HO decision algorithm, proposing a novel self-optimization algorithm based on adaptively changing HM and TTT according to the location, velocity, and signal-to-interference-plus-noise-ratio (SINR) of each user.

Our proposed algorithm adaptively selects the proper HM and TTT for each user according to its moving state. In modern networks, most cellular phones are easily embedded in global positioning system (GPS) services [8]. Hence, we can assume that both the location and velocity of the user are estimated, and thus, the status of the user velocity and its distance to each base station (BS) are easy to identify. Based

on the user's distance to both the serving and target cells, the HM can be computed adaptively. This can be done by mathematically formulating the HM's function of the reference signal received powers (RSRPs), considering that RSRP is a function of the user's distance to the BS, [5]. The computation of the HM's function is subject to a criterion such that the time average of the SINRs, measured relative to the serving and target cells over a specific time window, is larger than the pre-defined SINR threshold of the system to guarantee the avoidance of TLHOs and TEHOs. This is our first contribution, where the user's radio links to both its serving and target cells is strongly enhanced while the user equipment (UE) moves from its serving cell and goes inside the coverage of the target cell, aiming to achieve a successful HO. On the other hand, TTT is a parameter related to the time domain, and it is difficult to set it by detecting the user's location. For this, we support our algorithm by formulating a function that computes the TTT adaptively with each user velocity and its corresponding HM value obtained from the previous adaptive phase. This is done based on a geometric interpretation of the mechanism of the HO A3 event. Thus, the TTT values are completely related to the selected HM values for each user individually and according to their mobility state (velocity). This is what we consider as our second contribution in this paper, where a direct relationship between HM and TTT can be derived and used for the first time in this research field. As a result, the PPHO ratio can also be significantly reduced. The proposed algorithm implicitly deals with the overall HO cases, that is, macro-to-macro HO, macro-to-small HO, small-to-macro HO, and small-to-small HO.

II. RELATED WORK

In general, algorithms for making HO decisions between cells in a HetNet can be categorized based on several parameters related to the user and network topology. The decision part of any adaptive HO algorithm is the HO decision phase, which depends on the selection method of both HM and TTT values, that is, static, dynamic, or adaptive. Thus, the performance of the network is optimized. Here, it is meaningful for SON. In HetNets, the HO decision phase is always performed on the service cell side. The vast majority of the algorithms in the literature use a combination of different parameters to obtain the final HCP selection. As mentioned in [9], the main decision parameters for HOs between cells can be divided into five categories: **1)** velocity-based [10]–[17], **2)** received-signal-strength (RSS) or RSRP-based [18]–[24], **3)** cost-function-based [25]–[32], **4)** energy-efficient-based [33], [34], and **5)** interference aware, (e.g., SINR) [35]–[40]. Looking at the first category, one can find that either the moving direction of the UE is not considered, the mobility/network model is limited, or the small-to-small cell HO event is neglected. For the second category, we found that either the network structure is not a HetNet, or the number of HCPs is insufficient with regard to the system-level evolution perspective, that is, focusing either on HM selection or on TTT selection, but not both. On the other hand, the main disadvantage of the

cost-function-based HCP optimization algorithm's category is that the selection of weights combination is predefined by the authors, implying that there might not be adequate proof that these weights are the optimized weights. For the fourth category, either the authors only considered a single macrocell in their simulation or did not consider the interference power. Finally, looking at the fifth category, either the authors used a very limited coverage model for the small cells considering neither noise nor shadow fading, or the corresponding algorithm was checked by considering only the UHOs. Looking at recent relevant research from three years ago, we find that the work [41] proposes a cost-function-based algorithm. Although this scheme provides low PPHO and RLF HO ratios, the UE velocity is not suitable for high-velocity scenarios, that is, up to 300 km/h. Moreover, its algorithm cannot maintain a high HO success number and simultaneously reduces the PPHO ratio to a low level; that is, a conflict appears when the algorithm seeks to minimize TLHOs, TEHOs, and PPHOs simultaneously. The authors in [42] proposed a velocity-and-RSRP-based algorithm as an auto-tuning optimization algorithm to adjust the HCPs, but the SINR parameter was not considered. In addition, this work did not provide adequate proof of why the steps used to decrease or increase the TTT and HM were put in such a way. Furthermore, in [43], the same authors developed an RSRP-based algorithm without considering the velocity, which means that they published their new work [42] by simply adding the velocity decision parameter to their previous work in [43]. As a result, improvements were insufficient. However, in [44], a sensitivity analysis of both the HM and TTT thresholds was carried out for different network load levels and UE velocity. A fuzzy logic controller (FLC) that adaptively modifies the HM threshold, was proposed for HCP optimization [44]. Nevertheless, in [44], the PPHO ratio was not considered when evaluating the proposed algorithms. Among all the algorithms in this field, only the author in [9] discussed the HCP optimization problem in a very professional and accurate way, taking into account the overall reasons affecting the HO performance. His solution is simple and converges to reality. He presented in [9, CH.3-5] an algorithm using attractive performance thresholds for PPHO, SINR, and RLF HOs to enhance the HO decision by considering the velocity of the UE in selecting suitable and consistent HCPs. Unfortunately, the work in [9] did not discuss how to define these performance thresholds. In addition, the success of HO events depended only on a predefined RLF HO desired (approximately 27%). However, we will depend on some ideas in [9] to develop our novel algorithm. In fact, all HCP optimization algorithms in recent literature reviews, including [9], used the same technique, that is, HCP steps, to decrease and increase both the TTT and HM values, obtain the main goal of such algorithms (reducing PPHOs, TLHOs, TEHOs). Moreover, that was always without any discussion of why these steps were chosen in such a way. In this paper, we propose a completely new methodology for determining the suitable values of TTT and HM by establishing

a correlation between them, considering that each of the parameters of velocity, RSRP, and SINR is measured. This is done in a unified model to significantly reduce both the RLF HOs and PPHO ratios. Our proposed algorithm was investigated based on simulations of various scenarios using the MATLAB©2021a software. It is then compared with the [9], [42], [43], [48] algorithm and the classical setting of HCPs (i.e., fixed TTT and fixed HM). The results show that the proposed algorithm provides remarkable enhancements, as illustrated in Section VI.

III. SYSTEM MODEL
A. HetNet MODEL
We consider a HetNet scenario to be a multi-tier network structure consisting of multiple macro cells and multiple small cells deployed such that small cells are non-uniformly distributed relative to each macro cell. In this study, only the macro cell layout is considered to be wrapped around using a 19-cell-wrap-around hexagonal network topology with ultra-dense small cells. The small cell layout is not wrapped around. The 19-hexagonal macro cells are considered to be closely deployed in an urban environment in which the small cells are distributed randomly. The HetNet scenario is an important concept that has been widely used in LTE-A networks [9]. Small cells are normally considered to be microcells, picocells, or femtocells. For example, a three-tier HetNet consists of a mix of macro, pico, and femtocell BSs. In this study, we consider a two-tier HetNet considering a mix of macro and femtocell BSs. Generally, the range of small cells can range from ten to several dozen meters, and hence a small cell has a small range and low transmitting power (15 to 30 dBm) to work as Home evolved node BS (eNB) (HeNB). This small BS can be used to provide both indoor and outdoor broadband services [51]. As a trend, the densification of small-cell deployment will become popular in future network planning. The number of small cells can linearly increase network capacity. The considered 19-hexagonal macro cell model is consistent with real LTE-A HetNets deployed in an urban environment with high user density and traffic loads, including a small cell distribution [45]. Fig. 1(a) illustrates a general urban macro-cell scenario (without small cells), and Fig. 1(b) shows another scenario, considered with small cells as a simple example. We built consideration 19-hexagonal macro cells, 41-randomly distributed small cells, with 100-randomly distributed UEs in their primary positions in the environment (12000m × 12000m square area).

The total capacity of the considered system and users are significantly promoted by the use of small-sized BSs. The deployment of small cells improves the existing network capacity, although these low-power BSs overlap with existing macrocell networks. For the interference issues to be well addressed, Fig. 2 shows a top-down view of the entire simulation network system, which comprises a two-tier macro-small cell network (of the same type as that presented in Fig. 1(b), but with only 12 small cells, assuming a 1000m × 1000m
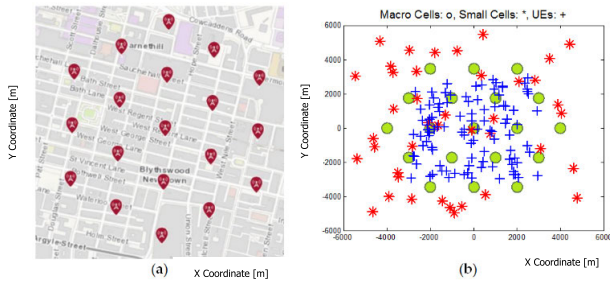
FIGURE 1. HetNet model, with 19 macro cells (o), 41 small cells (*), and 100 UEs (+), (a) urban macro-cell scenario [46], (b) MATLAB-based LTE-A urban macro/small-cell scenario.
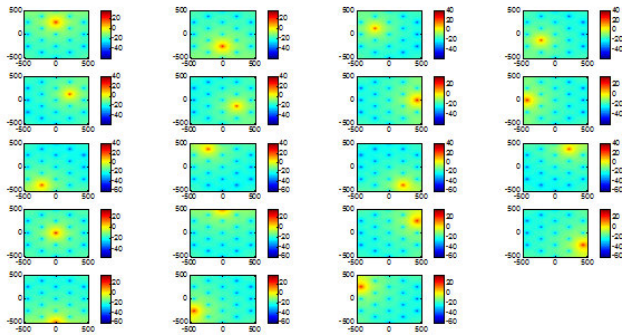

FIGURE 2. Top-down view of SINR map for each one of the 19 macro cells knowing that the RSRP of rest macro-BSs and of rest small-cells were considered to be interference power.

FIGURE 3. Top-down view of SINR map for each one of the 12 small cells knowing that the RSRP of rest small-BSs and of rest macro-cells were considered to be interference power.

square area). Fig. 2 shows a macro-SINR map. Fig. 3 shows a top-down view of the entire simulation network system to address the small-SINR map. We use the RSRP calculation to determine the current serving cell (either macro or small) and to calculate the corresponding SINR in each pixel (see Subsection C, where the procedures of SINR, RSRP, and interference map calculations are shown). The RSRP of the remaining BSs (non-serving cells) was considered to be the interference power. In both figures 2 and 3, it can be seen that different RSRPs created differential macro/small cell coverages. In addition, the different coordinates of the same type of BS (macro or small) also result in different coverages. Moreover, it is clear that the denser the deployed small cells, the higher the interference in the simulation environment.

This study mainly focused on the optimization of system-level HCPs. The growing density of small cells and the shortening of the cell radius have created various communication problems, among which the HO issue is one of the most challenging issues. By introducing the overlaid HetNet scenario in LTA-A, the aim of the HO function has to be evolved to further deal with maintaining connectivity and enhancing the performance of the entire network. In addition, owing to the small coverage and low transmission power, the HO procedure in HetNets is much more complicated and needs to be more intelligent. In this paper, we propose adaptive HCPs in HetNets (LTE-A) with dense small cells. Our proposed self-optimization algorithm based on adaptive HCPs is evaluated
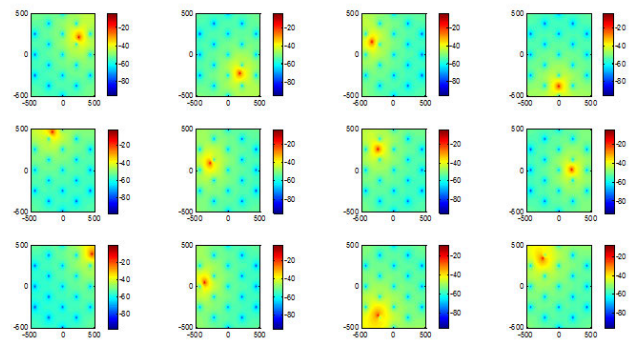
by simulation considering the HetNet scenario in the LTE-A system. Evaluating our algorithm considering 5G ultra-dense small cells (LTE-A and millimeter-wave networks) coexisting with the current networks is postponed as future work.

B. UEs MOBILITY MODEL

Figures 1(a), 2, and 3 have been created considering that all the UEs are in a static process, that is, they are all in the corresponding coordinates at a moment of time (fixed spatial positions). However, the HO according to A3 event is a dynamic process; that is, even if a UE moves out of the serving cell (macro or small cell) region and the maximum RSRP is obtained from a different cell (macro or small cell), the UE can still be served by the original serving cell. This is because it is not possible to have a successful HO (e.g., facing an RLF HO event), or the HO for the corresponding target cell is unnecessary (e.g., facing a PPHO event); otherwise, a successful HO would occur. In this study, we assume that the cell that provides the maximum RSRP is considered as the serving cell, while the remaining RSRPs are considered as interference-power-like cells. This assumption corresponds to the initial position of all the UE before each one moves to the next position in the environment. This is used to define the serving cell status initially. Then, for every new position, the candidate target (macro or small) cell will be selected corresponding to the maximum RSRP among the other cells (macro and small) excluding the current serving cell. Hence, a general mobility model for all UE needs to be developed.

In this study, we assume that each UE starts from an initial spatial point (x_0, y_0) in an environment with a random velocity v from the range (30 km/h to 300 km/h) given an initial random direction θ from $[0°$ to $360°]$. The UE keeps moving in this direction with the chosen velocity through a straight line until it reaches the boundaries of the environment (the four sides of a square whose area is 12000m × 12000m = 144 km², and the coordinates of the square 's heads are (6000m, 6000m), (6000m, −6000m), (−6000m, 6000m), (−6000, −6000)), in which the UE is set with another new random direction. Thus, it changes its mobility state according to this new direction and re-enters

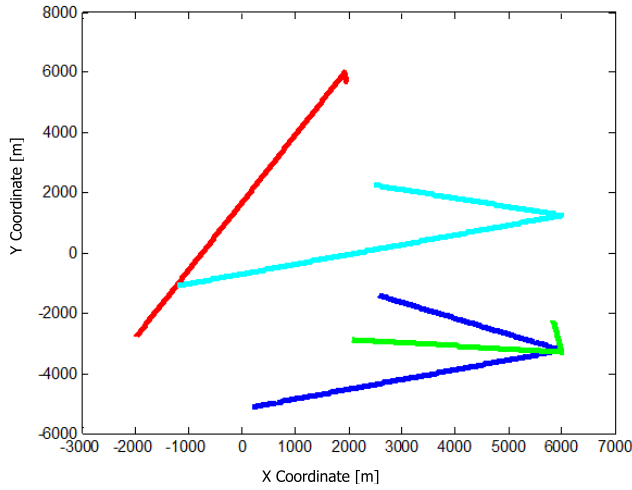the environment once again, moving through another straight line, and so on.

FIGURE 4. An example of 4 moving UEs in the simulation environment according to the considered mobility model.

Fig. 4. displays an example of such mobility model for 4 UEs moving with velocities 240, 240, 120, and 270 Km/h over 150 seconds, with a step of simulation time of 10 [ms].

C. SYSTEM METRICS

1) RSRP

In the HetNet case, the radio transmission system in small cells differs from its counterpart in macrocells. This is in terms of several parameters, including the RF transmitted power, RF frequency, and transmitting antenna gain [47]. Therefore, the free-space path loss model for a macro cell is different from that for a small cell. In this paper, we assume the following path loss gain scalar formula to represent the power loss resulting from electromagnetic wave propagation from a cell to the UE [5]:

$$PL_i^j = \frac{G_i^j G_0 \left(\lambda_{i,j}^2\right)}{\left(4\pi d_i^j\right)^2} \tag{1}$$

where the index j represents the correlation type of the cell relative to the UE that wants to perform an HO, (j = target cell, j = serving cell, or j = int (interference) cell), i represents the index of the RF type of the cell (i = small cell, or i = macro cell), G_o is the receive antenna gain of the UE, G_i^j is the transmit antenna gain of the cell (regardless of the value of indices i and j, i.e., macro-serving, macro-target, small-serving, or small-target), $\lambda_{i,j}$ is the corresponding signal wavelength, and d_i^j is the distance between the UE and the BS cell. In fact, the distance is a function of both ($x(t), y(t)$); the coordinates of the UE at time moment t and (x_i^j, y_i^j) are the fixed Cartesian coordinates of the cell. This distance function is expressed as

follows:

$$d_i^j \left(x(t), y(t), x_i^j, y_i^j\right) = \sqrt{\left(x(t) - x_i^j\right)^2 + \left(y(t) - y_i^j\right)^2} \tag{2}$$

Now, if we place P_i^j as the RF transmitted power from the BS cell, and put ζ_i^j to represent the shadow fading gain that follows a log-normal distribution with a zero mean and a standard deviation, σ, between 4 and 6 dB [6], [9], we can write the RSRP dB-formula of any UE as

$$RSRP_i^j(dB) = P_i^j(dB) - PL_i^j(dB) - \zeta_i^j(dB) \tag{3}$$

Equations (1) and (3) make it possible to distinguish between the RF broadcasts of small cells and that of the macro cells in HetNet.

2) SINR

By definition, the SINR calculated for each UE at any position ($x(t), y(t)$) and at any time moment t is the ratio of the received power from a cell (macro or small, serving or target) to the sum of the sum of the interference power of the rest of the cells (macro and small in the whole network) plus $P_{thermalnoise}$ the thermal noise power [6]. If the serving/target cell is a macro cell, we formulate the corresponding SINR in a scalar formula such that, (4), as shown at the bottom of the next page, or in a dB formula, (5), as shown at the bottom of the next page, where, (6), as shown at the bottom of the next page.

If the serving/target cell is a small cell, then we formulate the corresponding SINR in the same manner, that is, (7), as shown at the bottom of the next page.

In this paper, we formulate the thermal noise power (scaler) as $P_{thermalnoise} = K.T.B$, where K is Boltzmann's constant, T is the temperature of the UE RF receiver in Kelvin (298.15 K or above), and B is the bandwidth. The equations of the SINR presented above express the downlink SINR calculation in HetNet, where the SINR value is included in the measurement report (MR) created at the UE side every Δt (the simulation time step) during its motion through the HetNet.

D. SYSTEM PERFORMANCE INDICATORS

1) HANDOVER FAILURE RATIO (HOFR)

Successful HO executed from the current serving cell to another cell in the HetNet is conditioned by several factors [43]. First, the HO request (HRQ), performed from the serving cell to the main core of the HetNet in order to decide an HO execution, must not be a late request. This means that while the UE goes out of the coverage area of the original serving cell, there must not be an RLF event occurring in the radio link between the current serving cell and the user at a moment before the HO procedure is initialized. Otherwise, if it happens, it will imply multiple attempts by the UE to reestablish the connection with the target cell. This is actually the concept of a TLHO event caused by an RLF event in the serving cell. Second, the HRQ must not be an early

request. This means that when the user enters the coverage area of the target cell, there must not be an RLF event between the cell and the user at a moment after the execution of the HO procedure is completed. Otherwise, if it happens, it will imply multiple attempts by the user to reestablish the connection with the original serving cell. This is the concept of a TEHO event caused by an RLF in the target cell. If there are many TEHO and TLHO events during UE mobility, poor network performance in terms of mobility management is encountered. This might cause the connection to be dropped or interrupted; hence, many attempts have been made to reestablish the connection by the UE. Thus, the management of HetNet resources fails, and QoS deteriorates. The number of both TLHO and TEHO events indicates the performance of the system as a key performance indicator (KPI) in terms of the HO procedure execution. In this context, we put HPI_{HOF} as the first KPI, naming it the system performance indicator related to the RLF HO events. We define $HPI_{HOF}(t)$, for all the UE at each moment t, as the ratio of $NHOF_t$ (the total number of both TEHO and TLHO events) to NHO_t; the total number of HOs that have been executed at each moment t of the overall mobility of all the UE. The ratio $HPI_{HOF}(t)$ is given by the following equation:

$$HPI_{HOF}(t) = \frac{NHOF_t}{NHO_t} \qquad (8)$$

Equation (8) represents a ratio that calculates the number of RLF HOs divided by the total number of HOs for all UE at each new position (new moment) during their mobility. Thus, at the end of the simulation, one can observe the maximum or average (or whatever) number of RLF HOs relative to the total number of HOs executed. One of the main aims of any HO parameter optimization algorithm is to make $HPI_{HOF}(t)$ as small as possible at all times during the mobility of all UEs served by the HetNet. Almost all the previous algorithms in the literature (e.g., [9], [41], [43], [48]) defined HPI_{HOF} thresholds to be desired for the system, considering it as a predefined acceptable HPI_{HOF} limit in the overall performance.

We think that this methodology is weak; instead, we could dispense with the definition of thresholds of this kind, making our proposed algorithm in this paper more general.

2) PING PONG HANDOVER RATIO (PPHOR)

If both HM and TTT are not set correctly, it is possible that HO is successful but unnecessary at the same time, and vice versa. One common type of UHO is a ping-pong event. This event occurs if a call is handed over to a new cell and then is handed back to the original cell in less than the critical time (T_{crit}) that may rank from 1 to 6 s [6], [9], [41]. In particular, HetNets frequently suffer from the occurrence of this type of event, mainly because of the presence of small cells that have low geographical area coverage compared to those of macro cells. This situation often occurs in HetNets when the UE is handed over from a macro cell to a small cell. There is a high probability that the UE will be re-handed over to the same macro cell in less than T_{crit}, especially if the UE velocity is very high, or if both the values of both the HM and TTT control parameters are relatively small. In this context, we put HPI_{HOPP} as the second KPI considering it a system performance indicator related to PPHO events. We define $HPI_{HOPP}(t)$, for all the UE at each moment t as the ratio of $NHOPP_t$; the total number of PPHO events to NHO_t. The ratio $HPI_{HOPP}(t)$ is given by the following equation:

$$HPI_{HOPP}(t) = \frac{NHOPP_t}{NHO_t} \qquad (9)$$

Equation (9) represents a ratio that calculates the total number of PPHO events divided by the total number of HOs for all UE at each new position (new moment) during their mobility. Thus, at the end of the simulation, one can observe the maximum or average (or whatever) number of PPHOs relative to the total number of HOs executed. Another main aim of any handover parameter optimization algorithm is to make $HPI_{HOPP}(t)$ as small as possible at all times during the mobility of all UEs served by the HetNet.

$$SINR_{macro}^j = \frac{RSRP_{macro}^j}{\sum_{other\ macro\ cells} RSRP_{macro}^{int} + \sum_{all other\ small\ cells} RSRP_{small}^{int} + P_{thermal\ noise}} \qquad (4)$$

$$SINR_{macro}^i(dB) = RSRP_{macro}^j(dB) - RSRP_{macro-small}^{int+noise}(dB) \qquad (5)$$

$$RSRP_{macro-small}^{int+noise}(dB) = 10 \times \log_{10}\left\{ \sum_{other\ macro\ cells} RSRP_{macro}^{int} + \sum_{other\ macro\ cells} RSRP_{small}^{int} + P_{thermal\ noise} \right\} \qquad (6)$$

$$SINR_{small}^j = \frac{RSRP_{small}^j}{\sum_{other\ small\ cells} RSRP_{small}^{int} + \sum_{all\ other\ macro\ cells} RSRP_{macro}^{int} + P_{thermal\ noise}} \qquad (7)$$

The fundamental question that our manuscript answers is: How do we choose the suitable values of HM and TTT (the main HCPs) so that the HO decision is made successfully without leading to many events of type PPHO or RLF HO. This study proposes a new mechanism for setting the main HCPs of the HO decision procedure adaptively and according to event A3 (see the next section). It is HM that initiates, or not, the HO decision procedure, and it is TTT that terminates this procedure, resulting in either an HO action request being sent to the network controller core or not (see Equation (10)). Procedures that follow that decision procedure are those that consume network resources in transferring (or not) the coverage service for the UE to a new cell. Here, the decision to handing over the UE must be sound, and this mainly means that it should lead as lower as possible to PPHO or to RLF HO incidents. In this context, one could ask the following relevant question: Are there performance indicators, that is, KPIs, other than the number of PPHO (HPI_{HOPP}) or RLF HO (HPI_{HOF}) events? In fact, some studies (for example, [43]) use other performance indicators that are also considered important in evaluating the algorithm for selecting HCPs, such as throughput and interruption time. However, in this study, we consider that HPI_{HOPP} and HPI_{HOF} are the most important KPIs of significance in this field, following several other studies such as [9], [41], [42], [48]. We present our own justification for this, as follows:

First, many PPHO events will mainly lead to very low throughput, which reflects the low QoS performance of the system; therefore, the throughput indicator is a logical result of obtaining so many PPHO events. If the HO decision is controlled so as to be successful, leading to a reducing in PPHO events, it will logically result in improved throughput directly and without so many service interruptions. The throughput indicator is calculated during the implementation of the HO procedure. Here, we must differentiate between the HO decision-making procedure and HO execution procedure. The HO decision-making procedure depends on the measurement report (SINR, RSRP, and velocity information), as addressed in this study, while the HO execution procedure depends mainly on the method of allocating and controlling radio resources in the network, which is beyond scope of this study. More specifically, the HO execution procedure depends on radio resource control (RRC) messaging while imposing minimal impact on the application layer throughput during and after HO execution and completion. HO execution steps involve commanding the UE to the new radio resources, while HO completion involves releasing resources on the (old) source cell. Regarding the HO execution procedure, the RRC is responsible for judging whether the HO execution action is successful or not. Therefore, more PPHO events result in more consumption of network resources, thereby reducing the throughput and, increasing the overall average interruption time. Thus, one of the main aims of any HO decision mechanism is to reduce PPHO events, which mainly depends on the method of selecting both HM and TTT for each UE connected to the network. Thus, from a causal point of view, we say that when low performance in terms of throughput and interruption time is faced, a large number of PPHO events is one of the main reasons. If we reduce PPHO events, we will logically and naturally obtain good performance in terms of interruption time and throughput. Therefore, performance evaluation should be mainly dependent on the number of PPHO events occurring per the total number of HO events, which is literally the concept of HPI_{HOPP} in Equation (9).

Second, many RLF HO events will also lead to lower throughput and frequent outages. Therefore, we must again distinguish between events that cause another. they are TLHO and TEHO events that mainly lead to the wrong or failed HO decision and therefore the amount of information exchanged within the network system will be as little as possible per unit time (this is literally the meaning of the concept of low throughput). Thus, the evaluation of the HO decision algorithm must also be key with regard to TLHO and TEHO events (RLF HO events). This is because the performance with regard to these events results in the performance of the throughput indicator and the interruption or dropping of the call during the HO execution procedure. HO decision making (based on suitable HM and TTT selection) is what leads to such events regardless of the HO implementation procedure itself. The HO implementation is mainly not related to values HM and TTT, but rather to network resource allocation, and the UE itself represents another issue in terms of traffic management, which is beyond the scope of this study. As a result, the indicators for evaluating the HO decision mechanism (i.e., the mechanism for selecting the appropriate HM and TTT) must be separated from those indicators used to evaluate the HO execution procedure. Consequently, considering other KPIs such as throughput or interruption time in evaluating the model, in our opinion, do not add any reasonable value to the main aim of the work in the domain of this study.

IV. THE HO PROBLEM IN REGARD TO MOBILITY MANAGEMENT

Mobility management in cellular wireless networks is essential for providing seamless communication, depending on the UE's mobile situation. One of the responsibilities of radio resource management is to maintain radio link communication between the UE and the eNB, while the UE is in the coverage network area. This was achieved by implementing a successful cell-to-cell HO. Therefore, the success of the HO decision process is the process that establishes a new radio link connection from the current serving cell to another target cell in the network such that the channel outage or QoS is not affected [48]. Hence, mobile UEs maintain radio communication as they move within network coverage by performing a successful serving-to-target cell HO. The target cell provides better signal quality. Consequently, HO not only maintains connections in both HetNets and non-HetNets, but also improves both the performance of the entire network and the UE's QoS.

Classically, HO algorithms can be divided into three base categories: RSRP-based, RSRP with threshold, and HM/TTT-based [48]. In the first category, the HO decision is based only on the RSS. Thus, the HO is launched as soon as the RSS of the current serving cell deteriorates, and the RSS from the target cell is greater. For the second category, the HO decision is based on two necessary conditions that should hold together, by which the RSS from the serving cell is less than a certain predetermined threshold (i.e., HM), and that the RSS of the target cell is greater than that of the serving cell. Finally, for the third category, the HO algorithm initiates once the RSS of the target cell is greater than that of the serving cell plus the predetermined HM value; thus, this inequality holds for a predetermined specific time interval called TTT. The HM and TTT units were dB and ms, respectively. The HM and TTT values are chosen either statically for all over the UE or dynamically for each UE according to its mobility state. Making a robust HO decision is highly sensitive to selecting the HM and TTT values. The HCP values control the overall system performance, especially the HOFR and PPHOR. Intuitively speaking, the algorithm based on changing HM and TTT, as a self-optimization algorithm, with regard to the MRO issue, is the most practical and efficient technique for making an HO decision during UE motion [49]. We believe that any robust and hybrid algorithm, for example, thinking of a combination of two or more HO decision parameters such as RSRP, SINR, and velocity in one SON algorithm to adaptively select HCPs for each UE, may contribute to reducing the establishment of RLF HOs and UHOs. This was the primary aim of the present study.

Conventionally, the HO decision algorithm in LTE-A systems depends on the RSRP and is expressed mathematically as follows [50]:

$$RSRP_i^{\text{target}}(dB) \geq RSRP_i^{\text{serving}}(dB) + HM\ (dB)$$
$$for\ a\ time\ interval = TTT \quad (10)$$

The inequality in (10) clearly shows the role of both HM and TTT in determining the nature of the resulting HO event (whether it is successful HO, UHO, or RLF HO), regardless of the serving and target cells (macro-to-macro, macro-to-small, small-to-macro, or small-to-small). Generally, to make an HO decision, the RSRP of the serving cell should be continuously less than that of the target cell plus the HM during a TTT. Fig. 5 shows the effectiveness of varying the HM and TTT on the HO decisions [48] statically or adaptively. In this study, the HM and TTT values will be adaptively adjusted through two robust mathematical functions: **1)** to compute the proper HM depending on the RSRPs of both the serving and target cells, subject to robust conditions on the average time window of the SINRs of both the serving and target cells, and **2)** to compute the proper TTT in relation to the adaptive HM and velocity of the UE. This means that the HCP values are adaptively adjusted depending on several network factors, that is, RSRP, SINR, and UE velocity.
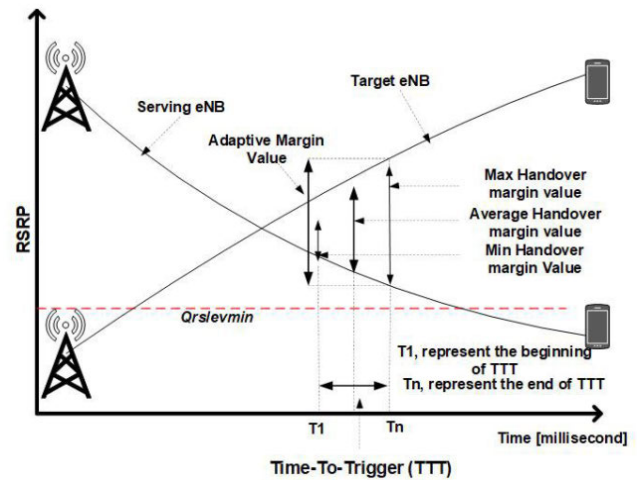

FIGURE 5. HO decision in LTE-A [48].

V. PROPOSED SOLUTION

Inequality (10) indicates that the HO decision depends mainly on three parameters: RSRP, HM, and TTT. The RSRP is a parameter related to the distance between the UE and cell. According to Equation (2), the distance depends on the location of the UE and the coordinates of the serving/target cell. Therefore, the network core cannot control the RSRP in the sense of optimization, because RSRP is "a parameter imposed" on the system and thus the system must work according to "its imposed value". Including RSRP into any possible algorithm is visible in the form of a **conditional constraint** that must be invested in determining the HCPs. On the other hand, HM and TTT are not imposed on the system; that is, the designer can control how they are selected. Thus, HCPs could be chosen based on tight criteria related to RSRP, SINR, or both, thereby ensuring the least number of unwanted events such as TLHO, TEHO, and PPHO.

Our first main idea is that the HM should be chosen in proportion to the coverage of both the serving and target cells intended to serve the UE according to **its relative locations varying with time.** As long as the UE is within a good coverage of its serving cell (i.e., the SINR is good), the value of HM must remain the same so that it should not be so small that inequality (10) is satisfied. However, when the UE reaches a good coverage range relative to another target cell, the HM should be chosen based on the properties of the coverage boundary between the current serving and target cells, for example, according to the ratio of the RSRP of the serving cell to that of the target cell. At the same time, both serving and target cells should provide good SINRs to ensure that there is no RLF HO. This is the basic idea that we will rely on in determining HM according to a function that fits the objectives mentioned above.

Our second main idea is that the TTT should be chosen according to the HM resulting adaptively, and according to the UE velocity at the same time. In the literature, the

corresponding algorithms select HM and TTT independently of the existence of any relationship between them. That is, it is assumed that there is no correlation between the HM and TTT. this study argues that this relationship is possible. In other words, the TTT value should not be chosen in isolation from the method of selecting the HM value, nor in isolation from the UE velocity value.

Therefore, by combining these two main ideas, an adaptive joint selection scheme for both HM and TTT could be developed, and a novel HetNet self-optimization mechanism based on individual UE mobility status could be discovered.

A. HM ADAPTATION MODEL

Generally, the smaller the HM value, the greater the probability that UHO events will occur; for example, a macro-to-small HO and then a small-to-the-same-macro-HO. However, larger values of HM can result in depriving the UE of a necessary and valid HO between two cells within the HetNet. In other words, if a large and fixed HM is selected for all UEs in the network (as traditional settings), the possibility of the UE entering into a new and better coverage area of a target cell will not coincide with the necessity of executing a successful HO event; hence, the UE could unfortunately remain connected to the original serving cell.

The HM selection for each UE seems to depend on the user distance to both the current serving cell and target cell. Therefore, according to Equations (1) and (3), the HM choice should be performed according to the relative relationship between the RSRP of the target cell and that of the current service cell, as long as each UE moves within the network, and this UE can exceed the boundaries of cell-to-cell coverage regardless of the cell type (whether it is a macro or small cell). In this way, the HM value of each UE mainly depends on the properties of the target cell and the serving cell (cell coordinates that determine the distances and hence the RSRPs), whether the target and the serving cells are of the same type (macro or small) or different (one is macro and the other is small).

We could define a mathematical principle of selecting HM according to the relative distances separating the UE from both the target cell and the current serving cell, or according to the ratio of the RSRP of these cells. In other words, the choice of HM could correspond to the ratio of the RSRP of both the target and serving cells, binding the UE to its serving cell as long as the UE is inside the serving cell coverage and will soon enter the target cell coverage. The UE is handed over to the target cell, taking the corresponding HM value, if and only if the SINRs of the UE with regard to both the serving and target cells are good in the sense of avoiding RLFs, and if the RSRP of the target cell is higher than that of the serving cell. In this manner, when the RSRP of the serving cell decreases (the UE distance to the serving cell increases), the HM value should be changed to a suitable boundary until the UE reaches the serving cell boundary and starts to enter the target cell coverage, that is, the RSRP of

the target cell increases (the UE distance to the target cell decreases). This leads to a suitable HM value when the UE is on the serving-target boundaries and exceeds the serving cell region. Because we do not want to lose the good coverage obtained from both the serving and target cells, that is, good SINRs are conditioned to avoid the occurrence of TLHO or TEHO events, the maximum decrease in HM value should be chosen. We interpret the HM chosen mechanism explained above using the following positivist conditional equation, (11), as shown at the bottom of the next page, where Θ is the SINR threshold that defines the channel outage probability of the system, W (typically 200 ms [5]) is a time window used to calculate the time average SINR that we use to compare with Θ to judge whether an RLF event occurs, $\text{HM}_{\text{max}} = 10$ the typical highest HM value used in the 3rd Generation Partnership Project (3GPP) standard [7], and t_k represents the moment of time at which the UE takes a new location in the network, where k is the index of the simulation step Δt. For the sake of clarification, if we choose Δt to be 10 ms, and if we want to simulate the model within 150 s, we will have 15000 simulation steps for the entire simulation, meanwhile W will correspond to 20 simulation steps, and t_k will initialize from the index $k = 21$, $t_{21} = 210ms$. Therefore, for each new location of the UE, we check the average values of SINR over a time window of length $W = 200ms$ corresponds to every previous 20 locations of the UE to compare with Θ, and checking for every new location, the RSRP values of both the target and serving cell, such that if the three conditions of Equation (11) are satisfied, the HM value is adapted to those RSRPs.

Equation (11) chooses the maximum value among the values corresponding to a range of moments in window W, where it maximizes the time-dependent function $\text{HM}_{\text{max}}\left(1 - \left(\frac{RSRP_i^{\text{serving}}(t)}{RSRP_i^{\text{target}}(t)}\right)^2\right)$ in $t \in [t_k - W, t_k]$. When the RSRP of the serving cell is always larger than that of the target cell, this time-dependent function always returns a negative value; hence, Equation (11) returns zero. When the RSRP of the target cell is equal to the RSRP of the serving cell, then, at the next moment, the target cell likely starts to provide a larger RSRP than the current serving cell; hence, there will be a probable HO decision that might be made. From here, we are interested in selecting HM so that the result is subject to three severe constraints commensurate with the requirements of the system. The maximum value is chosen if and only if all three conditions are satisfied. That is, obtaining the idiosyncratic HM of each UE accurately depends on the fulfillment of the three inequalities: **1)** $\underset{t \in [t_k - W, t_k]}{\text{mean}}\left(SINR_i^{\text{target}}(t)\right) \geq \Theta$, **2)** $\underset{t \in [t_k - W, t_k]}{\text{mean}}\left(SINR_i^{\text{serving}}(t)\right) \geq \Theta$, and **3)** $RSRP_i^{\text{serving}}(t) \leq RSRP_i^{\text{target}}(t)$. When one of these three inequalities is not satisfied, for example when $RSRP_i^{\text{serving}}(t) > RSRP_i^{\text{target}}(t)$, $\forall t$ whatever the SINRs are, the Equation (11) returns 0, because

the quantity $\text{HM}_{\text{max}} \left(1 - \left(\frac{RSRP_i^{\text{serving}}(t)}{RSRP_i^{\text{target}}(t)} \right)^2 \right)$ will equal to a negative values all time, and this means that the UE will still be served by the original serving cell, and there is no need for this UE to be handed over to another cell in the network. In any case, the adaptive HM will inevitably be positive and in the range from 0 to 10 dB for all users in the network, and over the entire simulation time.

It is clear that the value of HM defined in Equation (11) is specific to each UE according to its individual mobility state within the network. Here, it is the meaningful of "idiosyncratic" adaptation of HM, which is one of the HCPs. From here, it can be said that our mechanism of selecting the HM is adaptive, and it determines the HM according to the UE's mobility state, to the fixed locations of cells in the network, and to the cell type (small or macro).

B. TTT ADAPTATION MODEL

The mobility state of the UE in the network is determined by its distance to each BS and its velocity. In the previous subsection, we suggested a mechanism for determining the appropriate HM value for each UE in the network according to its successive positions during its motion. In this subsection, we will develop a mechanism to determine the value of TTT based on the corresponding value of HM, as well as based on the UE velocity. We assume here that the TTT value must be suitable for the time-varying motion system of each UE, and it must be related to the selected HM. In other words, instead of changing the values of TTT and HM independently based on an increase or decrease in their values by unjustified steps as in the literature, we define here the pairs (HM, TTT) based on a relationship that correlates the TTT and HM values with each other; at the same time, this relationship is derived from the properties of the time-varying motion system of each UE.

We treat this issue as follows. Assume that a user moves within the coverage of its current serving cell with velocity v [m/s] and moves away from this cell to approach the coverage area of a target cell of the same network. When the inequality condition of (10) is satisfied, that is, the condition of the HO triggering event A3 is satisfied, the TTT timer starts counting. Thus, if the inequality continues to hold for a period equal to TTT, the user will have moved a distance of $v \times \text{TTT}$ [m]. According to 3GPP TS 36.331, the values of TTT are

typically chosen from a set of 16 different values, that is, as 3GPP specifies, in [7]. TTT values are taken from {0, 40, 64, 80, 100, 128, 160, 256, 320, 480, 512, 640, 1024, 1280, 2560 and 5120 in [ms]}. This also means that the TTT could change from 0 to 5.12 [s]. We then have 16 different distances for the same UE. These different distances for the same user imply different SINR values.

If a large fixed value of TTT is chosen, then the inequality condition in (10) requires a long period of time to be fulfilled during which the user will become within the target cell coverage area and very far from the original serving cell. This may lead to a TLHO event as long as the UE distance to the original serving cell will have been significantly reduced, and hence the corresponding SINR. On the other hand, if a small fixed value is chosen for TTT, there is a high probability of the occurrence of the PPHO event, as long as the inequality condition of (10) will require a small period of time to remain true. Moreover, there is a high probability of the occurrence of the TEHO event where the user may not have become in sufficient coverage area of the target cell to have a sufficient SINR in this situation; thus, the communication between the user and the target cell may be broken even if the HO process to the target cell is completed. In both cases, the value of the user velocity affects the occurrence of undesired events (TLHO, TEHO, and PPHO), because different velocities will imply different distances according to different values of TTT, and hence lead to an extreme decrease in system performance if a fixed TTT is selected regardless of both the UE velocity and the suitable HM.

We note here that, depending on the value of TTT (whether large or small), and on both the UE velocity and the HM, a trade-off of a special type must be considered between having good performance with respect to the TLHO (having a few TLHO events by selecting a small TTT) with poor performance with respect to both the TEHO and PPHO events (having many TEHO and PPHO events due to small TTT), and vice versa. From this point of view, any mechanism of choosing TTT should consider both the user velocity and the corresponding suitable HM such that good overall performance can be obtained (having a few TLHO, TEHO, and PPHO events at the same time).

Therefore, in this study, we assume that the value of TTT must be basically adaptive to the velocity of the user, and must also be basically adaptive to the adaptive HM developed

$$
\text{HM}_{\text{adaptive}} = \max_{t \in [t_k - W, t_k]} \left\{ 0, \text{HM}_{\text{max}} \left(1 - \left(\frac{RSRP_i^{\text{serving}}(t)}{RSRP_i^{\text{target}}(t)} \right)^2 \right) \right\}
$$

$$
\text{subject to} \begin{cases} \displaystyle\operatorname*{mean}_{t \in [t_k - W, t_k]} \left(SINR_i^{\text{target}}(t) \right) \geq \Theta, \\ \displaystyle\operatorname*{mean}_{t \in [t_k - W, t_k]} \left(SINR_i^{\text{serving}}(t) \right) \geq \Theta, \\ RSRP_i^{\text{serving}}(t) \leq RSRP_i^{\text{target}}(t) : t \in [t_k - W, t_k] \end{cases} \tag{11}
$$

in the previous subsection. In the following, we explain the adaptive mechanism for selecting the TTT value according to this assumption.
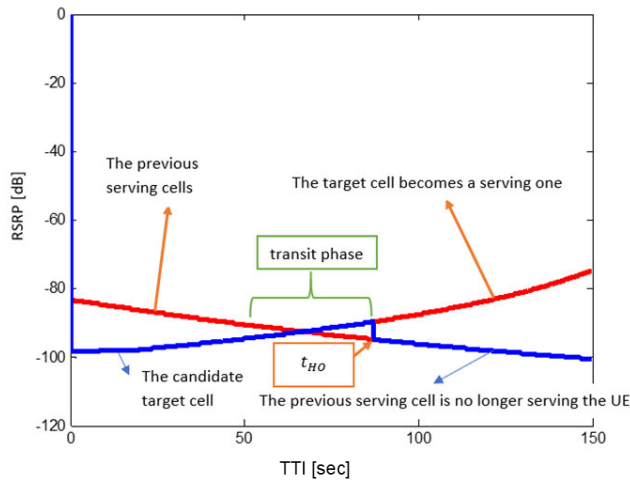

FIGURE 6. An illustration of a successful HO event with corresponding terms.

Fig. 6 shows the RSRPs obtained from both the serving cell and the target cell during the movement of a user with a velocity of 30 km/h within HetNet consisting of 19 macro cells and 41 small cells (femtocell), with TTT = 480 ms and HM = 5 dB. Fig. 6 assumes that HO has been executed and the UE has been handed over from the macro cell number 15 to the macro cell number 12, where this HO is initialized at moment $t_{HO} = 87.10$ s and started to triggered at the moment $t_0 = 86.62$ s, i.e., $t_{HO} - t_0 = $ TTT $= 480$ ms. We plotted Fig. 6 such that the red and blue colors represent the serving and target cells, respectively. This representation is considered before HO is executed. When HO is executed, the serving cell status of the UE changes between the two cells, and the color of the RSRP curve changes at that moment when the HO decision has been made. The target cell becomes a serving cell and takes the new red color, while the UE is no longer linked to the previous serving cell, which is plotted in blue.

The moment t_0 corresponds to the first time that the inequality in (10) is fulfilled; that is, at t_0, we have

$$RSRP^{target}_{macro12}(t_0) \geq RSRP^{serving}_{macro15}(t_0) + 5[dB].$$

The moment t_{HO} corresponds to the last time the inequality of (10) is fulfilled, and this corresponds to the moment when the HO process is initialized; that is, at t_{HO}, we also have

$$RSRP^{target}_{macro12}(t_{HO}) > RSRP^{serving}_{macro15}(t_{HO}) + 5[dB].$$

If we zoom in the plot area around the HO decision event in Fig. 6, we obtain Fig. 7. Fig. 7 shows the transition of the serving cell state from macro cell **No. 15** to macro cell **No. 12** at $t_{HO} = 87.1$ s, and it also shows the moment t_0.

In Fig. 7, points A, B, C, and D correspond to the values $RSRP^{target}_{macro12}(t_0)$, $RSRP^{serving}_{macro15}(t_0)$, $RSRP^{target}_{macro12}(t_{HO})$ and
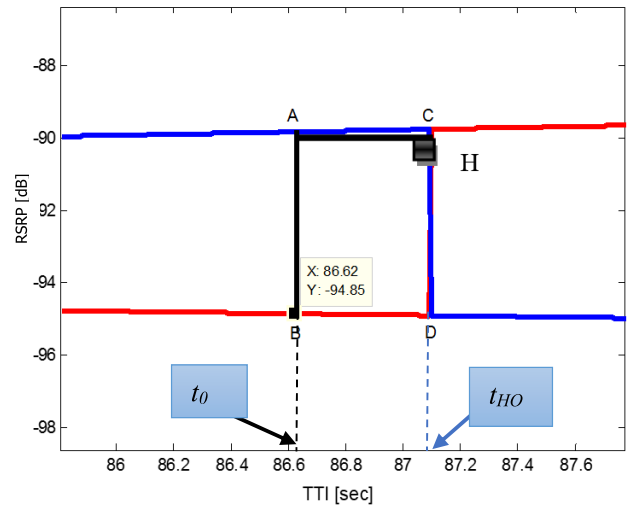

FIGURE 7. An illustration of zooming in Fig. 6 around the HO region.

$RSRP^{serving}_{macro15}(t_{HO})$, respectively. In this regard, we can propose the following:

$$\text{diff}_1 = RSRP^{target}_{macro12}(t_0) - RSRP^{serving}_{macro15}(t_0)$$
$$\text{diff}_2 = RSRP^{target}_{macro12}(t_{HO}) - RSRP^{serving}_{macro15}(t_{HO})$$

Here, we notice, according to (10), that:

$$\text{diff}_2 > \text{diff}_1 \geq \text{HM}.$$

Hence, we can easily put:

$$\text{diff}_1 = \alpha_1 \times \text{HM}; \quad \alpha_1 \geq 1, \text{ and diff}_2 = \alpha_2 \times \text{HM}; \quad \alpha_2 > 1$$

where α_1 and α_2 are real positive numbers.

On the other hand, the point H in Fig. 7 represents the point of intersection of the line segment $||AH||$ perpendicular to the line segment $||CD||$, starting from point A. Without affecting the generality, our main idea here, regarding the issue of HO, is to focus on the geometric properties of the quadrilateral ABCD obtained in Fig. 7. Quadrilateral ABCD generally represents a non-isosceles trapezoid. In ABCD, we can see that diff$_1$ and diff$_2$ correspond to the lengths of the parallel sides $||AB||$ and $||CD||$, respectively. In addition, if we study the RSRP plot (Fig. 6) as a function of the distance traveled by the UE in the network environment, the height of the ABCD $||AH||$ can be directly proportional to the quantity $v \times$ TTT, by multiplying the time axis in Fig. 7. by velocity. Thus, we could write:

$$||AB|| \equiv \text{diff}_1 = \alpha_1 \text{HM},$$
$$||CD|| \equiv \text{diff}_2 = \alpha_2 \text{HM}, \quad \text{and}$$
$$||AH|| \equiv v \text{TTT} \Rightarrow$$
$$\text{Area Of ABCD} = \frac{||AB|| + ||CD||}{2} ||AH||$$
$$\equiv \frac{\alpha_1 + \alpha_2}{2} v \times \text{HM} \times \text{TTT} \quad (12)$$

From Equation (12), We notice that v, HM, and TTT could be correlated to each other via the time-varying UE

state. The RSRPs of the UE relative to both the current serving cell and the target cell change with time while the UE keeps moving through the network. Hence, we can say that Equation (12) can confirm that there might be a reasonable correlation between the UE velocity and the HCPs: TTT and HM. This means that any choice of the pair (HM, TTT) for each UE should consider such a relationship. Elucidating the existence of this relationship is the most important contribution of this study. For the sake of simplification, we can assume that the area of the trapezoid ABCD is constant for each valid HO. This means that the successful HO should correspond to the same area of this trapezoid with regard to both the current serving cell and target cell states. Therefore, the pair (HM, TTT) for each UE could be chosen such that the ABCD area remains approximately constant for each HO executed on an individual UE. From this perspective, we can consider the choice of an adaptive TTT such that there might exist a nonlinear regression model between the variable TTT and the variable $(1/(v \times HM))$, assuming that the normalized area of the ABCD takes the following formula:

$$\text{Normalized Area Of ABCD} = \frac{\text{Area of ABCD}}{\frac{a_1 + a_2}{2}}$$
$$\propto Constant, \text{ such that :}$$
$$Constant \propto v \times HM \times TTT \Leftrightarrow TTT$$
$$\propto \frac{1}{v \times HM} \qquad (13)$$

In this context, we look for a formula that can represent the relationship between TTT and HM via v. For this, we could consider a proper nonlinear regression model that determines the adaptive value of TTT according to the adaptive value of HM obtained from Equation (11) and at the same time according to the UE's velocity v. To do that, we start from Equation (12), where it is obvious that the range of the resultant adaptive HM values is [0,10] dB, which corresponds to 3GPP TS 36.331, [7]. On the other hand, the values of the UE velocity we want to study in this study are in the range [0,300] km/h. Because the values of TTT should be obtained discretely from the set {0, 40, 64, 80, 100, 128, 160, 256, 320, 480, 512, 640, 1024, 1280, 2560, and 5120 in [ms]}, or continuously, TTT $\in$ [0,5.120] [s], we used Microsoft Excel to obtain such a nonlinear regression model between TTT and $1/(v \times HM)$).

Table 1 shows the typical data of HM, TTT (3GPP TS 36.331, [7]), and v values that correspond to the range of velocities we want to study in this paper. In Table 1., we also provide the corresponding values of quantity $(1/(v \times HM))$. The main reason for arranging the data in Table 1 in this manner (HM and TTT are both small, or both large in columns 1 and 5) is that we want to have a special kind of relationship between HM and TTT through a given value of velocity v. This is explained as follows:

First, regarding the data arrangement in columns 1 (HM data) and 5 (TTT data) of Table 1, we want the pairs (HM, TTT) to be such that HM and TTT are both small or both large. This means that one element of this pair (e.g., HM)

is not required to be large, whereas the other (i.e., TTT) is small at the same time. This criterion is more compatible with the requirements of the HO procedure in a network. If the HM is large and the TTT is small, it is possible to deny the user from better coverage of the target cell than the current serving cell. This means that it is possible to have a target cell that fulfills the inequality (10) condition with a small TTT to achieve it. Therefore, a smaller HM value should be obtained. On the other hand, if the HM is small and the TTT is large, then we are facing the possibility of a large number of PPHO, which will negatively affect the performance of the network in terms of loading a cell with many users more than this cell can.

Second, regarding the data arrangement in column 2 (v data) and columns 3 and 4 ($v \times HM$ and $1/(v \times HM)$ data). On the one hand, we look for a relationship between TTT and $1/(v \times HM)$, intuitively desiring a hyperbolic relationship between v and TTT; that is, small values of TTT are desired to correspond to large values of velocity, and vice versa. This idea is obtained by analogy with equation (13). In addition, this idea is an important system requirement because higher UE velocities will increase the distance $v \times TTT$; therefore, there is a high possibility of TEHO or TLHO events. On the other hand, the reason for forming data of $v \times HM$ in this manner is also intuitively derived from the ABCD area relationship in Equation (12), because we are looking for a relationship between TTT and $v \times HM$.

TABLE 1. Typical data of TTT, HM, and UE's velocity.

HM [dB]	v [km/h]	$v \times HM$	$1/(v \times HM)$	TTT[s]
1.00	20	20.0	0.050000	0.040
1.50	35	52.5	0.019048	0.064
2.00	50	100.0	0.010000	0.080
2.50	65	162.5	0.006154	0.100
3.00	80	240.0	0.004167	0.128
3.50	95	332.5	0.003008	0.160
4.00	110	440.0	0.002273	0.256
4.50	125	562.5	0.001778	0.320
5.00	140	700.0	0.001429	0.480
5.50	155	852.5	0.001173	0.512
6.00	170	1020.0	0.000980	0.640
6.50	185	1202.5	0.000832	1.024
7.00	200	1400.0	0.000714	1.280
7.50	215	1612.5	0.000620	2.560
8.00	230	1840.0	0.000543	5.120

using Microsoft Excel$^{©}$ (see the Appendix) and plotting the TTT data vs. $1/(v \times HM)$ data and checking **a suitable trendline** (**Power Type**) equation, we obtain Fig. 8. Fig. 8 illustrates the robust relationship between TTT and $1/(v \times HM)$. As a result, we propose such a relationship, as the following equation represents the desired adaptive TTT with both the adaptive HM value obtained from (11) and the velocity v:

$$\mathbf{TTT_{adaptive} = 0.001}\left(\frac{1}{v \times HM_{adaptive}}\right)^{-0.974} \qquad (14)$$

We notice that Equation (14), by some sense of the relationship between HM and TTT via v, is approximately equivalent
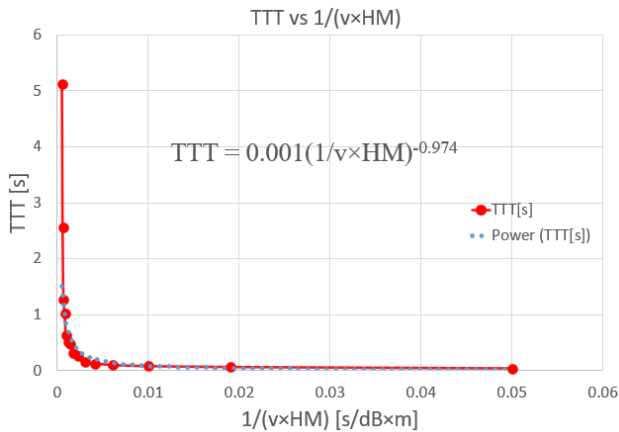
FIGURE 8. The proposed nonlinear regression model of TTT vs. 1/(v*HM).

to Equation (13). We call this model *the hyperbolic model of the relationship that governs the correlation of the TTT with both HM and velocity*. Mathematically, when Equation (11) returns 0 exactly, (i.e., $HM_{adaptive} = 0$ dB), the corresponding value of TTT seems to be undefined or undetermined. To solve this numerical problem, we assign 0 to $TTT_{adaptive}$. Logically speaking, this assignment will not affect the validity of the model as long as the zero value of HM will result from the RSRP of the current serving cell being always larger than that of the target cell. Thus, event A3 corresponding to inequality (10) cannot occur regardless of the value of TTT, as long as HM is always 0, and inequality (10) will not be achieved at all. In fact, in this case, we can also choose a large value for TTT, say 5120 ms, or even any large value, because in this case whatever TTT is, inequality (10) will not be true at all times.

C. ON THE METHODOLOGY OF DERIVING THE HCPs EQUATIONS

The methodology adopted in this study was new and promising. This methodology focuses on finding a correlation of some kind between the HM and TTT, so that the setting of each is related to the other in the HO decision. We investigated the system requirements that essentially reduce PPHOs and RLF HOs (TLHOs and TEHOs) and addressed the issue that HCPs should be chosen in such a way that the trade-off between reducing the number of TLHOs and the number of both TEHOs and PPHOs at the same time could be resolved. Using Equations (11) and (14), this trade-off can be easily resolved. The way of thinking that we follow in this paper is based on positivist methodology. We analyze the system requirements to obtain success and necessary HOs to avoid RLF HOs (e.g., TLHOs and TEHOs) or UHOs (e.g., PPHO). These requirements are achieved by making a sound HO decision based on valid and suitable values of both HM and TTT depending on both the velocity and location of both the moving UE and stationary cells in the network.

Generally, the cell boundary is easy to define in a one-tier macro-cell scenario because the radius of the macro cell

coverage can be defined. However, in the two-tier HetNet scenario, small cells are normally deployed in the existing macro cells. Thus, it is difficult to determine the cell coverage by considering only the radius information of the macro or small BS or both. The RSRP is a distance-based variable, as shown in Equations (1) and (3). Thus, we could say that choosing adaptive HM values could be based on considering the distance of the UE to its serving cell and the distance to the target cell boundary, that is, the UE's location. The main idea of an adaptive HM is to allow the HM to achieve a suitable value when the UE approaches the target cell boundary from the coverage of the current serving cell. Assuming that the UE is moving from the serving cell (macro or small) to the target cell (macro or small), the HM will reach a suitable value in the sense of desired PPHO, TLHO, and TEHO performance when both the RSRP and SINR of the target and serving cell satisfy the corresponding conditions. The purpose of the chosen HM mechanism using Equation (11) is to bind the UE to its serving cell even if it is inside the target cell coverage such that the possibility of obtaining a TLHO, TEHO, or PPHO is minimal.

Moreover, it is the SINR that determines the validity of the radio link between the user and the serving cell. If, during the communication process, SINR is less than a certain threshold, the communication will be broken with a high probability; otherwise, the user will continue to communicate with the serving cell. We have already referred to the threshold Θ in Equation (11). In addition, by definition, the radio link of the communication is described as good in modern systems if and only if the SINR value is greater than the threshold Θ within a time window of length 200ms. Otherwise, there is an outage and we say that there is a failure in the radio link, that is, an RLF event [5]. TLHO-type or TEHO-type HO events are undesirable in the context of HO decision issues. The TLHO event occurs when a failure occurs in the radio link between the user and the serving cell before the HO decision to the target cell is initiated [43]. Therefore, it is said that there is a late HO where the user is in a situation where the radio link communication between the UE and the current serving cell is weak and the HO process is not completed. The TEHO event occurs when a failure occurs in the radio link between the user and the target cell before the HO decision to the target cell is completed [43]. Therefore, it is said that there is an early HO where the user is in a situation where the radio link communication between the UE and the target cell is weak and the HO process is not completed. From this point of view, we establish the conditions of Equation (11) so that the SINR for both the target cell and the current serving cell are considered in the HM decision. This prevents both TEHO and TLHO from occurring simultaneously.

On the other hand, the main objective of presenting equation (12) is to illustrate the existence of a relationship between HM and TTT. This is the focus of our main idea in this paper, which revolves around a new way of adapting the values of HCPs by considering such a relationship. The x-axis in Fig. 7 represents the time axis. Multiplying the time axis

of Fig. 7 by the UE velocity quantity, that is, velocity × time, we obtain the distance the UE travels between t_0 and t_{HO}. This traveled distance is also related to the location of the UE relative to a cell BS, which is a target or serving one. The y-axis in Fig. 7 represents the RSRP axis, and we know that RSRP is a function of distance, as shown in Equations (1) and (3). In this way, we interpret the quantity $v \times$ TTT as equal to the length of the linear segment $||AH||$, which represents the height of the trapezoid ABCD in Fig. 7. This is explained as follows: Point B in Fig. 7 represents the moment of time t_0 at which the inequality in Equation (10) ($\text{diff}_1 \geq$ HM, i.e., A3 events or the HO trigger event) is satisfied for the first time for a user moving at a speed of v in the network environment. Point D in Fig. 7 represents the moment of time t_{HO} when the inequality in Equation (10) ($\text{diff}_2 >$ HM, i.e., A3 events or the HO trigger event) is satisfied for the period of time TTT [s] for the same user in the network. Here, it is how we came out with both v and $v \times$ TTT. Regarding the alpha1 and alpha2 quantities, we previously stated that they are real positive numbers such that we place $\alpha_2 > 1$ and $\alpha_1 \geq 1$ in order to mathematically convert the inequalities $\text{diff}_2 >$ HM and $\text{diff}_1 \geq$ HM into equalities, that is, to rewrite them as $\text{diff}_2 = \alpha_2 \times$ HM and $\text{diff}_1 = \alpha_1 \times$ HM. At the moment t_0, diff_1 will be greater than or equal to HM, while at the moment t_{HO}, diff_2 will be **exactly** greater than the HM; thus, we put the two real positive numbers $\alpha_2 > 1$ and $\alpha_1 \geq 1$. In contrast, from the trapezoid ABCD, we can see that diff_1 and diff_2 are the lengths of the parallel sides, that is, the two linear segments $||AB||$ and $||CD||$, respectively. Here, it is how we came out with alpha1,2. Finally, we derive equation (12) using the law of the area of the trapezoid ABCD.

Equation (12) only shows the possibility of a relationship between HM and TTT, but it is not directly applied in this study. Instead, we extrapolated a similar relationship between these HCPs in response to system requirements to obtain the minimum number of PPHO, TEHO, and TLHO events. This is consistent with the analysis proposed in Subsection 2 of Section V. The Appendix shows the simple steps for obtaining Equation (14) using Microsoft Excel©. Although this methodology appears to be very simple, or even naïve, in developing a specific mechanism for assigning TTT values, it is promising and leads to desirable results in this regard. Moreover, the method requires **no steps** to adjust the HCP values according to the methods described in the literature. Simply, we initially set an adaptation mechanism for HM by means of positivistic Equation (11), and by the requirements of an appropriate value of TTT that must be considered for each UE according to its speed and HM value, we organized Table 1, and inferred a possible relationship between HM and TTT, as shown in Equation (14). In the Results section, we show the time-varying curve of both HM and TTT for several users moving in the network at different velocities.

D. EVALUATION THE PROPOSED SOLUTION
The HO decision algorithm proposed in this study is based on adaptive HM and TTT values for each UE with many decision parameters such as RSRP, SINR, and velocity. These decision parameters are all included in the MR periodically sent to the system. The HM value for each UE is adaptive to both the RSRP and SINR using the positivist Equation (11). The TTT value is adaptive to the adaptive HM and to the velocity of the UE analogically to the positivist Equation (14).

The robustness of Equation (11) is that it accurately determines the appropriate HM values for each UE according to the time average of its SINR over a time window whose width is exactly equal to the width used to determine the outage channel probability in the system. Equation (11) also determines that the appropriate HM according to the RSRPs obtained from both the current serving cell and the target cell once the user enters the coverage area of the target cell and its distance to the serving cell increases.

On the other hand, the robustness of Equation (14) is evident from the fact that: First, it is derived from the analysis of the HO procedure in a comprehensive manner. Second, it is derived from the assumption that there should be a relationship between the values of TTT and HM, such that the velocity parameter is considered in such a relationship. In fact, even in the real world, assuming a more realistic model that takes into account the fast-fading or shadow-fading phenomena of the communication channel, **1)** the trapezoid ABCD consideration remains realistic and exists, **2)** the heads of such a trapezoid still represent true RSRP values received from both the target cell and the current serving cell, **3)** the trapezoid ABCD height also remains proportional to the distance $v \times$ TTT; and **4)** the lengths of the two bases of the trapezoid ABCD (the small one $||AB||$ and the large one $||CD||$) remain multiples (alpha1 and alpha2) of the value HM at both moments t_0 and t_{HO}.

Our intention in referring to the trapezoid ABCD is only to show the possibility of a correlation between HM, TTT, velocity, and the rest of the system parameters. This seeks to establish such a relationship to develop a more realistic SON algorithm that controls the HO procedure in the network. In addition, Equation (14) is fully consistent with the analysis in [9, CH-5.3] regarding the relationship between the TTT should be selected and the UE velocity. Although the proposed solution in [9] includes selecting the TTT values according to the assumption of a prior threshold value for HOFR, Equation (14), in this study, dispenses with any performance threshold assumption of this type. Moreover, Equation (14) considers the relationship between TTT and v including HM, whereas in [9], only a relationship between TTT and velocity is proposed. Furthermore, in the Results section, we find that both HOFR and PPHOR ratios will be very close to zero using Equations (11) and (14), and the resultant performance is much better than that of [9], and even better than other related works on SON algorithms such as [42], [43], [48].

In fact, another relationship could be obtained to select an adaptive TTT based on both the HM and velocity. Sorting the data in column 3 of Table 1 (i.e., $v \times$ HM data) from largest to smallest, and using the same sorting of the TTT data (from
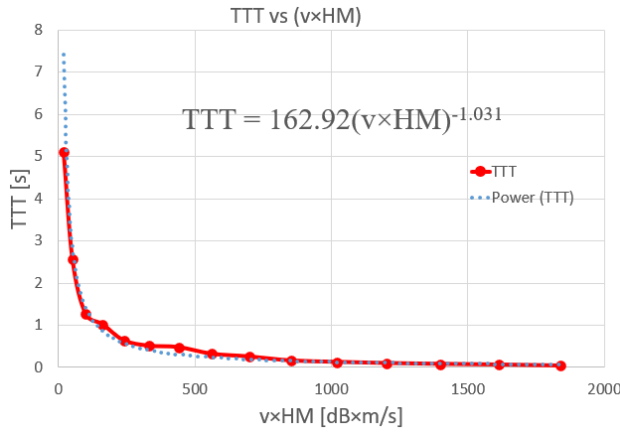
FIGURE 9. Another proposed nonlinear regression model of TTT vs. (v × HM).

smallest to largest), and then exploring another nonlinear regression model using Excel, we obtain Fig. 9. Fig. 9 is somewhat similar to the curve shown in Fig. 8. We again obtain the following **power-liked trendline** equation fitting this TTT new curve as follows:

$$\text{TTT}_{\text{adaptive}} = 162.92 \left(v \times \text{HM}_{\text{adaptive}} \right)^{-1.031} \quad (15)$$

Equation (15) is also equivalent to Equation (14) and can also be used to select an adaptive TTT for each UE. It is interesting to point out that if we round the exponential -1.031 to -1 in Equation (15), we obtain the product $v \times \text{HM}_{\text{adaptive}} \times \text{TTT}_{\text{adaptive}}$ to be constant as if it represents a constant ABCD area, and equivalently similar by analogy to the statement in Equation (13).

E. THE PROPOSED ALGORITHM: SON BASED ON ADAPTIVE HM AND TTT

Algorithm 1 describes the proposed adaptive HCP-based SON algorithm. Using this algorithm, the mobile UE is handed over according to the A3 event mechanism if and only if the RSRP of the target cell is greater than the RSRP received from the current serving cell, and if the average SINR, over a time window W, computed relative to both of those cells, is sufficient in the sense that it is greater than the outage channel connection threshold Θ. Thus, the values of HM and TTT are determined according to this criterion and are completely adapted to the user's mobility status. Then, based on these adapted values, the HO process is executed. If the HO procedure is completed, the user is served by the target cell; otherwise, the current serving cell continues to serve him/her while he/she is in the HetNet. This algorithm does not require any performance thresholds to control the TEHO, TLHO, or PPHO events, as in most studies. Moreover, it greatly reduces the ratios of those events, as we will see in the Results section.

Algorithm 1 is a novel distributed SON algorithm that adaptively chooses HCPs based on user velocity, RSRP, and SINR. The choice of HM (Equation (11)) depends on

---

Algorithm 1 : SON Based on Adaptive HCPs
___

1. Initialize HetNet' parameters (Powers, BS Locations, Losses, Fading, Gains, . . . etc.)
2. Inputs: Θ, W
3. Output: HM, TTT and HO decision for each UE moving in the environment
4. Detect the current serving cell and the target cell periodically
5. Collect MR information for each UE (RSRPs, SINRs, v, location) periodically
6. **LOOP**: for each UE
7.   **If** the conditions of equation (11) are satisfied **then**
8.   Compute $\text{HM}_{\text{adaptive}}$ according to equation (11) for the UE
9.   Compute $\text{TTT}_{\text{adaptive}}$ according to equation (14) or (15) for the UE
10.   **If** the inequality in equation (10) is satisfied by $\text{HM}_{\text{adaptive}}$ for $\text{TTT}_{\text{adaptive}}$ **then**
11.   HO decision ← True
12.   Send HRQ
13.   Execute HO
14.   Complete HO procedure
15.   Handover the UE to the target cell
16.   **else**
17.   HO decision ← False
18.   Run HO Trigger Timer
19.   The current serving cell remains the same
20.   **end if**
21.   **Else**
22.   HO decision ← False
23.   The current serving cell remains the same
24.   **end if**
25. **end LOOP**
___

the location of the UE in the sense that both RSRP and SINR are calculated by considering the distances between the UE and cells in the network. The choice of TTT (Equations (14) or (15)) depends on the UE velocity and the adaptive HM chosen.

The distributed SON entity is equipped at each eNB in the network to collect related data and periodically optimize the HCPs for each UE according to its mobility status. Each UE receives the requested traffic over either small eNB (SeNB) or macro eNB (MeNB) cells. The cells use the X2 interface to communicate with each other during the HO decision procedure [7]. This procedure is supported by the X2 interface, which can exchange operational reports, parameter configurations, and RLF status. At each SeNB and MeNB, a distributed SON collects the HO information to optimize HM and TTT using Equations (11) and (14). The HO action is executed when the UE moves from the serving cell region to the neighboring cell regions. The serving cell decides to hand over that UE to the candidate target cell following the MR that the UE periodically sends to its current serving cell before the HO decision is made.

VI. SIMULATION RESULTS

Table 2 illustrates the simulation parameter settings. We simulated the proposed algorithm by considering six scenarios and evaluating the resultant performance. For each scenario, we use different values of the parameters X, N, and ST, such

that the first five scenarios consider $T_{crit} = 6$ s (the worst case regarding the PPHO issue) as in [9], and for the sixth scenario, we assume $T_{crit} = 2$ s as in [42], [43], [48]. In the first five scenarios, we compared our algorithm with [9] and the classical setting, and ran the algorithms of [42], [43], [48] for the sixth scenario. Only the author in [9] reviewed the issue of adaptive HM and TTT values in LTE-A HetNet, while the rest of the references studied the issue of auto-tuning HM and TTT values according to predetermined steps without evidence of why these steps were chosen in this way. The concept of adaptation fundamentally differs from the concept of auto-tuning (or adjusting). The adaptation technique somehow means setting the values of the HCPs in proportion to the values of the decision-making parameters (RSRPs, SINRs, velocity) by using a function robustly defined. Auto-tuning simply reset the values of the HCPs according to the steps that are not firmly defined. To compare the performance with the classical cases of HCP settings (fixed HCPs), we consider the data in Table 3.

We followed [9, Table. 3-1] in setting most of the system simulation parameters, including the bandwidth of the LTE-A HetNet system model scenario assumed in this study, where the authors of [9] studied the same system model scenario. In addition, we followed [42] in setting the HO execution time to 50 ms.

It is important to point out here that it is true that the HetNets scenario makes radio resource management in macro-small networks challenging, but it is another aspect in designing the overall system. However, macro cells and small cells in HetNets share the available radio resources, which means that they share the available bandwidth, from 1.25 MHz to 20MHz, in LTE release8 [54, p.24]. Thus, the bandwidth value of 10MHz is suitable for the LTE-A HetNet scenario. This bandwidth could be shared between all cells in the network topology (LTE-A or even 4G) [53].

It is also true that this sharing may cause cross-layer interference and co-layer interference. It would have been interesting to explore this aspect, but it is beyond the scope of this study because our proposed model focuses on selecting a pair of values for HM and TTT for each user based on RSRP, velocity, and SINR. To simplify the simulation, we want to indicate that the simulated model only considers the interference power by calculating the SINR for each user at any position and at any time moment, (see Equation (4)). In addition, in the 5G HetNet model, macro cells and small cells operate on different carrier frequencies only to avoid interference [43], but in our LTE-A HetNet scenario, as in [9, Table 3-1], we consider one value of carrier frequency for both macro and small cells.

On the other hand, one could argue that a large bandwidth should be used for small cells, but this is true only if the HO decision algorithm is simulated for a 5G network, where high radio carrier frequencies (for example, from the Ka-band) and very high bandwidth up to 1 GHz should be considered. However, we examine the proposed HO decision algorithm using the case of LTE-A HetNets, as in [9], where the macro cells are distinguished from small cells with regard to the transmitted power value and hence in regard only to the coverage area.

TABLE 2. System simulation parameters [9], [42], and [53].

Simulation Parameter	Value
Macro Cell Layout	19 Cells, Hexagonal Grid, Wrap-Around on area of 6 Km×6 Km
Small Cell Layout (N)	41, 91 cells randomly deployed on area of 9 Km×9 Km
Carrier Frequency	2 [GHz]
Bandwidth [9,53]	10 [MHz]
Macro Cell Tx Power	46 [dBm]
Small Cell Tx Power	24 [dBm]
Macro Cell Tx Antenna Gain	10 [dBi]
Small Cell Tx Antenna Gain	10 [dBi]
UE Rx Antenna Gain	10 [dBi]
Channel Fading Phenomena	A log-Normal distribution-based Shadowing with zero mean and 5 dB standard deviation
UE Deployment (X)	1000, 2000, 3000 users randomly deployed
UE Velocity (v)	In range of 30 to 300 Km/h randomly chosen for each UE
Simulation Time (ST), Lifespan	ST= 150, 250 [s] ⇔ Lifespan =15000, 25000 rounds
Transmission Time Interval (TTI), i.e., Simulation Step Time $\Delta t = t_k - t_{k-1}$, k=1,2,3,4, …, Lifespan	TTI= Δt =10 [ms]
SINR averaging window (W)	200 [ms]
SINR threshold (Θ)	-35 [dB]
Critical Ping-Pong Handover Time (T_{crit})	2, 6 [s]
Handover Execution Time [42]	50 [ms]
Simulation Area (Mobile Users)	12 Km×12 Km
HM	Adaptive
TTT	Adaptive
Initial UEs Locations (x_0,y_0)	Randomly chosen in Simulation Area
Initial UEs Directions θ_0	Randomly chosen from $[0,2\pi]$
Mobility Model for Each UE $(x(t_k),y(t_k))$	$x(t_k)= x_0+v\times\cos(\theta_0)\times t_k$ $y(t_k)= y_0+v\times\sin(\theta_0)\times t_k$

TABLE 3. Common classic cases of fixed setting for the HCPs.

No. Case	HM [dB]	TTT [ms]
Case 1	2	100
Case 2	4	256
Case 3	6	480

A. SCENARIO 1 (X = 1000, N = 41, ST = 150, T_{crit} = 6)

For 1000 UEs moving at different speeds within 150 s, considering 41 small cells, Fig. 10 shows the rate of occurrence of PPHO events in relation to the total number of HO events executed. Fig. 11 shows the rate of occurrence of RLF HO events (TLHOs, TEHOs) in relation to the total number of HO events executed. The previous two figures show that the performance of the proposed algorithm is much better than the classical method that uses constant values for both HM and TTT, as well as much better than the algorithm in [9]. On the time-average of the ratios $HPI_{HOPP}(t)$ and $HPI_{HOF}(t)$, the
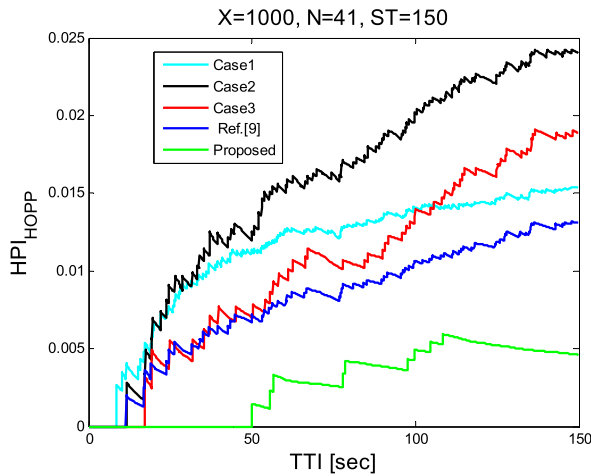
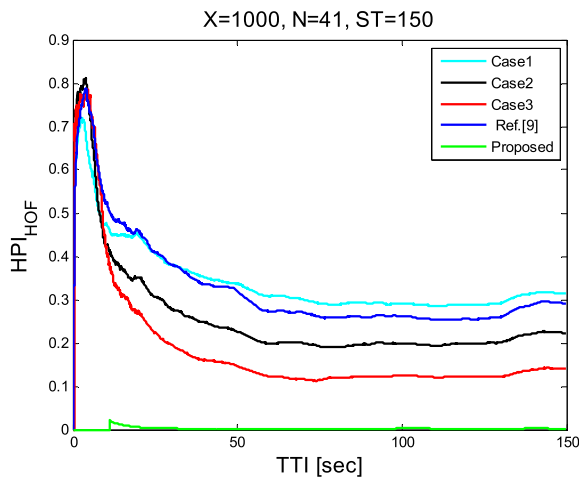**FIGURE 10.** PPHOR results of the scenario 1, X = 1000, N = 41, ST = 150 [s], T$_{crit}$ = 6 [s].

FIGURE 11. HOFR results of the scenario 1, X = 1000, N = 41, ST = 150 [s], T$_{crit}$ = 6 [s].

PPHOs and RLF HOs have rates of 2 and 3 per thousand, respectively. By running [9], we obtained 33% for HOFR and 1% for PPHOR. In particular, we observe from Fig. 11. that there are cases of conventional settings in which the performance in terms of immunity against RLF HOs is better than that of [9]. This result is normal because the algorithm in [9] is limited by a predefined RLF HO threshold, and there is no standard to define that threshold in a fundamental way. This implies the possibility of the existence of better instances of fixed settings for the HCPs compared with [9]. We find a similar result for the rest of the scenarios presented in this section.

Table 4 shows a brief summary of the results in this scenario, where the high performance of the proposed algorithm can be observed in terms of very few PPHOs and RLF HOs. For 1000 HOs executed within 150 s, there are only two PPHOs, and there are only three RLF HOs by running the proposed solution, and there are 10, 13, 20, and 10 PPHOs

and 330, 340, 260, and 160 RLF HOs considering the solution of [9], and the classical cases 1st, 2nd, and 3rd, respectively.

TABLE 4. PPHOR and HOFR performance of the first scenario.

	Proposed	[9]	Case1	Case2	Case3
$\underset{t\in[0,ST]}{\text{mean}}(HPI_{HOPP}(t))$	0.002	0.01	0.013	0.02	0.01
$\underset{t\in[0,ST]}{\text{mean}}(HPI_{HOF}(t))$	0.003	0.33	0.34	0.26	0.16
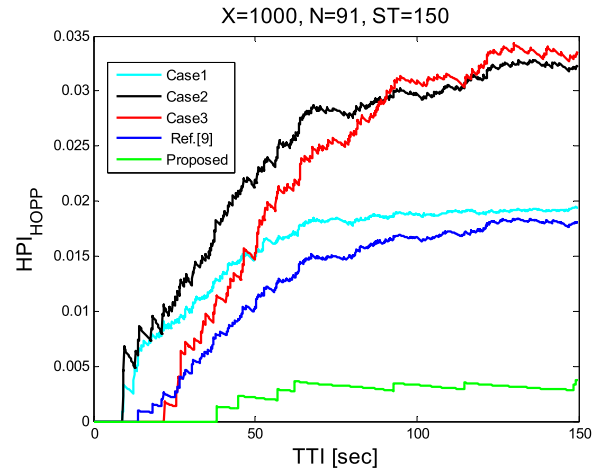
FIGURE 12. PPHOR results of the scenario 2, X = 1000, N = 91, ST = 150 [s], T$_{crit}$ = 6 [s].
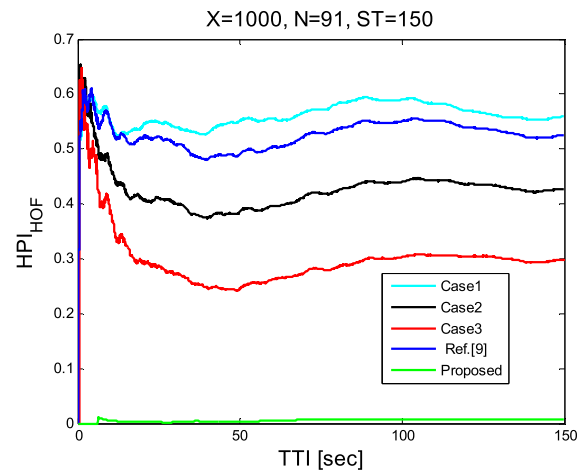
FIGURE 13. HOFR results for, X = 1000, N = 91, ST = 150 [s], T$_{crit}$ = 6 [s].

B. SCENARIO 2 (X = 1000, N = 91, ST = 150, T$_{crit}$ = 6)

For 1000 UEs moving at different speeds within 150 s, considering 91 small cells (much more than that in the first scenario), Fig. 12 shows the PPHOR time-varying curve, whereas Fig. 13 shows the HOFR time-varying curve. Figures 12 and 13 again show the high performance of the proposed algorithm. The PPHOs and RLF HOs occurred at rates of only two and five per thousand, respectively. This

was obtained although the number of small cells in HetNet increased from 41 to 91 for the same number of UEs and for the same simulation time. Therefore, we conclude that even for a larger number of small cells, which naturally implies more ping-pong (of type: macro-to-small HO and then small-to-macro HO), the proposed algorithm is impervious to both PPHO and RLF HO events.

Table 5 shows a brief summary of the results in the second scenario, where the high performance of the proposed algorithm can also be observed in terms of very few PPHOs and RLF HOs. For 1000 HOs executed within 150 s, there are only two PPHOs, and there are only five RLF HOs by running the proposed solution, and there are 12, 15, 23, and 21 PPHOs and 525, 561, 425, and 298 RLF HOs considering the solution of [9], and the classical cases 1st, 2nd, and 3rd algorithms, respectively.

TABLE 5. PPHOR and HOFR performance of the second scenario.

	Proposed	[9]	Case1	Case2	Case3
$\underset{t\in[0,ST]}{\text{mean}}(HPI_{HOPP}(t))$	0.002	0.012	0.015	0.023	0.021
$\underset{t\in[0,ST]}{\text{mean}}(HPI_{HOF}(t))$	0.005	0.525	0.561	0.425	0.298
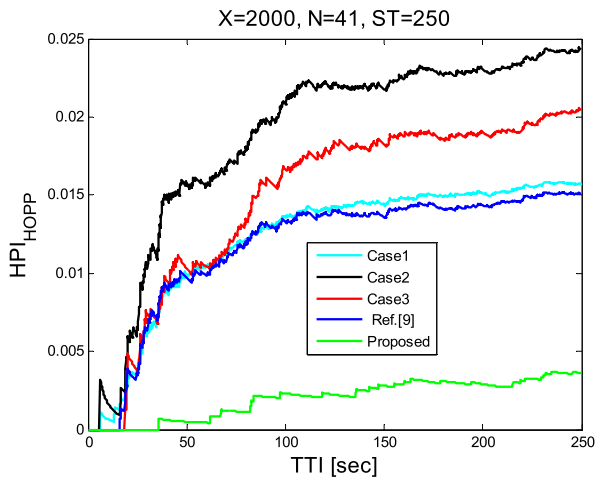
FIGURE 14. PPHOR results of the scenario 3, X = 2000, N = 41, ST = 250 [s], T_{crit} = 6 [s].

C. SCENARIO 3 (X = 2000, N = 41, ST = 250, T_{crit} = 6)

Figures 14 and 15 show the time-varying plots of PPHOR and HOFR, similar to figures 10, 11, 12, and 13. Here, we increase the number of UEs and make them move within time *ST* more than in the previous scenarios for the same HetNet configuration. Again, we note from figures 14 and 15 the robustness of the proposed algorithm and its immunity against UHOs and RLF HOs. This is obtained although the number of users has doubled compared to the previous two scenarios, and the simulation time has nearly doubled. This implies that the proposed algorithm maintains the same performance.
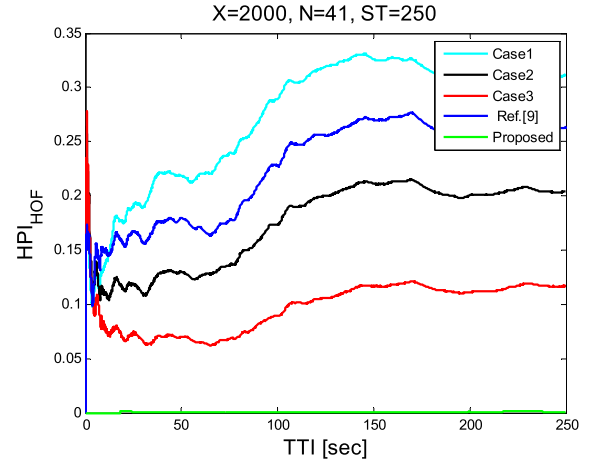

FIGURE 15. HOFR results of the scenario 3, X = 2000, N = 41, ST = 250 [s], T_{crit} = 6 [s].

Table 6 shows a brief summary of the results of this scenario, where the high performance of the proposed algorithm can also be observed in terms of very few PPHOs and RLF HOs. Here, for 10000 HOs completed in the network within 250 s, there are only 20 PPHOs, and there are only six RLF HOs by running the proposed solution, 120, 120, 190, and 150 PPHOs and 2500, 2700, 1800, and 980 RLF HOs considering the solution of [9], and the classical cases 1st, 2nd, and 3rd algorithms, respectively.

D. SCENARIO 4 (X = 2000, N = 91, ST = 250, T_{crit} = 6)

Now, we consider the same settings as in the third scenario, but with a larger number of small cells. We notice that

TABLE 6. PPHOR and HOFR performance of the third scenario.

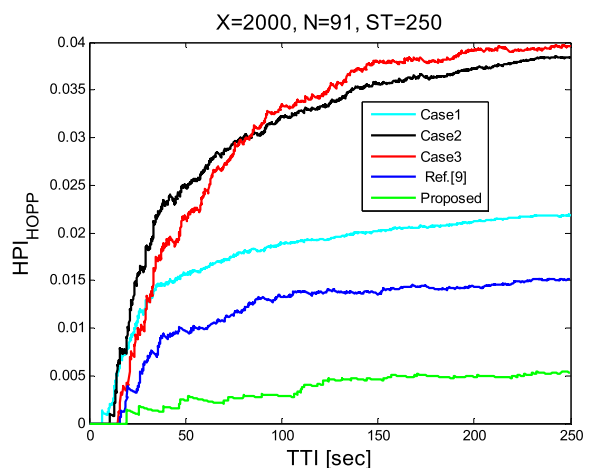|	Proposed	[9]	Case1	Case2	Case3
$\underset{t\in[0,ST]}{\text{mean}}(HPI_{HOPP}(t))$	0.002	0.012	0.012	0.019	0.015
$\underset{t\in[0,ST]}{\text{mean}}(HPI_{HOF}(t))$	0.0006	0.25	0.27	0.18	0.098

FIGURE 16. PPHOR results of the scenario 4, X = 2000, N = 91, ST = 250 [s], T_{crit} = 6 [s].

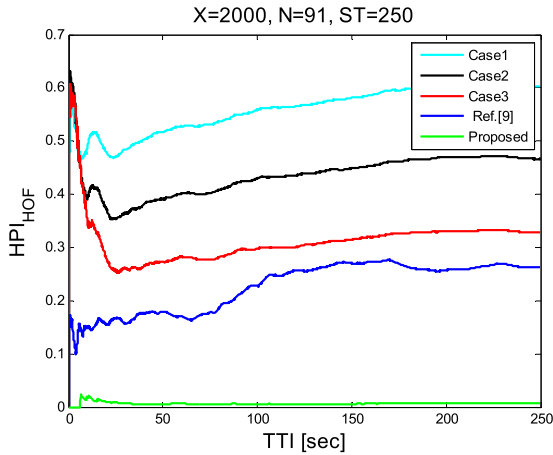**FIGURE 17.** HOFR results of the scenario 4, X = 2000, N = 91, ST = 250 [s], T_{crit} = 6 [s].

FIGURE 18. PPHOR results of the scenario 5, X = 3000, N = 91, ST = 150 [s], T_{crit} = 6 [s].

our algorithm maintains a significantly better performance, as shown in figures 16 and 17. Table 7 again confirms the robustness of the proposed algorithm in comparison with fixed HCPs and [9]. This means that the performance of our algorithm is affected neither by an increase in the number of users nor by an increase in the number of small cells, and this performance is maintained even with prolonged mobility of all users.

TABLE 7. PPHOR and HOFR performance of the fourth scenario.

	Proposed	[9]	Case1	Case2	Case3
$\underset{t\in[0,ST]}{\text{mean}}(HPI_{HOPP}(t))$	0.003	0.012	0.017	0.03	0.03
$\underset{t\in[0,ST]}{\text{mean}}(HPI_{HOF}(t))$	0.0006	0.23	0.56	0.44	0.31

E. SCENARIO 5 (X = 3000, N = 91, ST = 150, T_{crit} = 6)

Now, we consider a scenario that represents as the worst case compared to the previous scenarios. We consider 3000 users moving again at varying velocities and facing 91 small cells for a period of time equal to 150 s. As shown in figures 18 and 19, we note the high performance of the proposed algorithm even with a larger number of users and a larger number of small cells. As shown in Table 8, the number of PPHOs is nine per ten thousand, and the number of RLF HO events is 61 per ten thousand, which is a near-perfect performance compared to the traditional setting of HCPs and that of [9].

F. SCENARIO 6 (X = 1000, N = 91, ST = 150, T_{crit} = 2)

The previous scenarios dealt with a critical time situation to calculate the number of PPHO events, as the worst case, that is, T_{crit} = 6 s. It is well known that the greater the T_{crit}, the greater the number of PPHOs, given that a greater T_{crit} increases the probability of re-handing over the UE to the original cell in a sufficient time. In this scenario, we
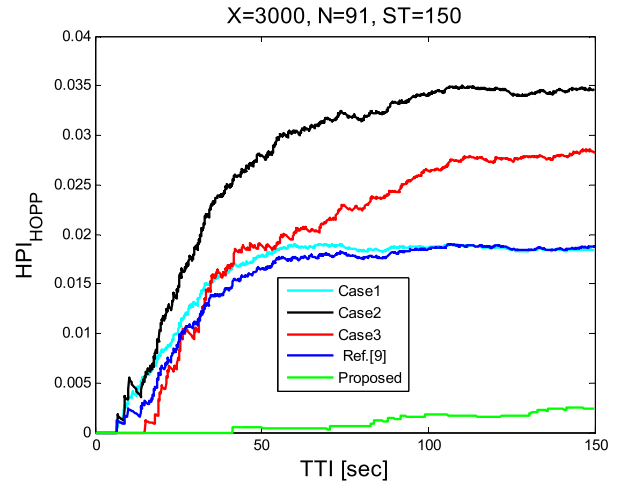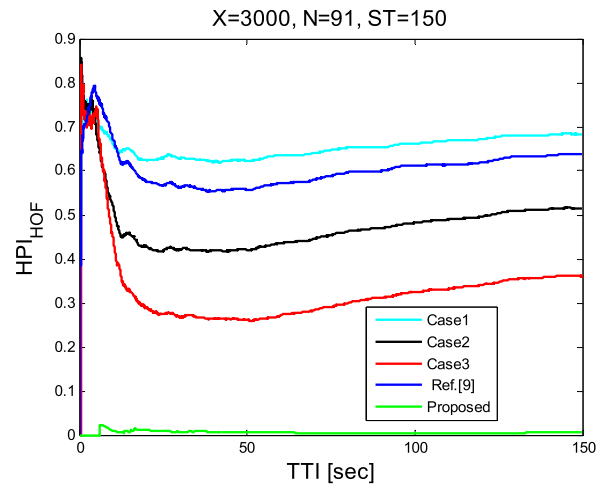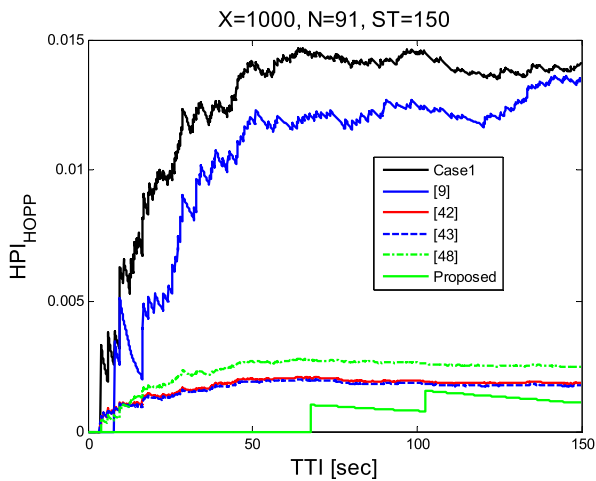

FIGURE 19. HOFR results of the scenario 5, X = 3000, N = 91, ST = 150 [s], T_{crit} = 6 [s].

TABLE 8. PPHOR and HOFR performance of the fifth scenario.

	Proposed	[9]	Case1	Case2	Case3
$\underset{t\in[0,ST]}{\text{mean}}(HPI_{HOPP}(t)$	0.0009	0.015	0.016	0.027	0.019
$\underset{t\in[0,ST]}{\text{mean}}(HPI_{HOF}(t))$	0.0061	0.60	0.65	0.47	0.33

consider a critical time smaller than the worst case, that is, we choose T_{crit} = 2 s, considering 1000 UEs moving within 150 s, and facing 91 small cells. At first glance, the number of PPHOs will certainly decrease compared to the previous scenarios, but the proposed algorithm remains very effective. By running the algorithms of [42], [43], [48] within our environments and obtain the results represented as plots, Fig. 20 shows the rate of occurrence of PPHOs in relation to the total number of HO events executed. Fig. 21.

shows the rate of occurrence of RLF HO events in relation to the total number of HO events executed. These two figures show a comparison of the performance of our proposed algorithm with the algorithms of [9], [42], [43], [48], but our algorithm considers a more general user mobility model. In this scenario, we assume a medium speed $V_r = 90$ km/h, as in [42], [48], and the threshold of RLF HO is equal to 1% as in [48] and 27% as in [9] with HM and TTT steps of 1 dB and 50ms, respectively, as each of those algorithms assumed.

FIGURE 20. PPHOR results of the scenario 6, X = 1000, N = 91, ST = 150 [s], T$_{crit}$ = 2 [s].
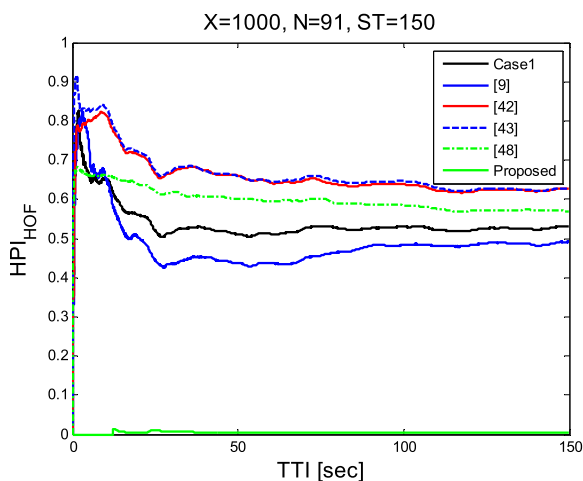
FIGURE 21. HOFR results of the scenario 6, X = 1000, N = 91, ST = 150 [s], T$_{crit}$ = 2 [s].

Figures 20 and 21 show unequivocally that the algorithms proposed in [9], [42], [43], and [48] do not solve the trade-off problem between PPHOs and RLF HO reduction simultaneously. As shown in Fig. 21, the adaptive algorithm of [9] is better than all algorithms (except ours) in terms of the HPI$_{HOF}$, but at the same time it gives worse performance compared to the other algorithms in terms of the HPI$_{HOPP}$, as shown in Fig. 20. Similarly, algorithms [42], [43], [48] perform well in terms of ping pong but, at the same time,

fail to match the same quality to obtain a good performance in terms of RLF HO. As a comparison between these algorithms, we find that the algorithm [48] is better than those of [42], [43] in terms of RLF HO. This is because the algorithm in [48] considers a performance threshold for the RLF rate in determining the appropriate HCP values, but it gives worse performance than [42], [43] in terms of PPHO. In addition, Fig. 21 clearly illustrates that there might be a classic case using fixed HCPs (case1) that results in a better RLF HO performance compared with each algorithm of [42], [43], [48], although an RLF threshold is used in [48], although the main claim of both [42], [43] is that their proposed algorithms outperform all classic cases. Hence, this is a clear indication that the solutions provided by these algorithms will not always be good, knowing that [42] and [48] consider a strict set of velocities to evaluate the performance. In this paper, we consider a more general mobility scenario where we assume the UEs to move at arbitrary velocities in the range from 30 km/h to 300 km/h without the need to assume a medium velocity V_r, as proposed in [42], [48]. Moreover, we note that the algorithms of [42] and [43] give approximately the same performance for each curve in figures 20 and 21. This is normal because the algorithm in [42] is just a slight increment over the work of [43] proposed by the same authors. In [42], only velocity and RSRP (without SINR) were considered in the mechanism of determining the HCPs. In addition, the general conditions and HCP steps of the original algorithm in [43] remained the same in its updated version in [42]. On the other hand, our proposed algorithm gives a very good performance for both indicators, and thus it is more capable of solving the trade-off issue, as is clearly evident from figures 20 and 21. It has the ability to simultaneously minimize both PPHOR and HOFR. This results in a very good reduction over time for both KPIs. The ability of our proposed algorithm is demonstrated by the robustness of the equations considered in the selection of HM and TTT. It is very important to show here that the comparison is based on the selection of $T_{crit} = 2$ [s] for both our algorithm and the algorithms in [9], [42], [43], [48]. Generally, evaluating any SON algorithm by considering $T_{crit} = 2$ s is not sufficient. considering $T_{crit} = 2$ is definitely a small time to study the problem of PPHO as long as the nature of this event itself is directly related to this quantity of time. If T_{crit} is very small, for example, 2 [s], there will certainly be very few PPHOs, even with classical HCP settings. The best then is to evaluate algorithms with a critical time greater than that. By running this scenario frequently for $T_{crit} = 6$ [s], we notice that the performance of [42], [43], [48] degrades significantly with respect to PPHOs. However, our algorithm maintains good performance for this worst-case scenario as Figures 10-19 show. On the other hand, these algorithms only process the user mobility for a very specific set of values, and assume a non-essential way to assign HM and TTT values without justifying how the corresponding steps are chosen, and without justifying how to choose the threshold value for the HOFR. Therefore, our proposed algorithm can

be described as a global algorithm in this research field, which takes into account any potential user speed from 30 to 300 km/h without the need to define any threshold for PPHOR or HOFR, and without the need to adjust HCPs by using steps. Finally, figures 22 and 23 illustrate how the adaptive HM and TTT change over time and velocity, respectively. These two figures result from the simulation of the current scenario, where there are 1000 users moving in the network environment. Because showing HM and TTT curves for all 1000 users would be futile (not evident in one figure), we randomly chose five users to obtain figures 22 and 23. We note from figures 22 and 23 that specific values of HCPs are given for each user and according to its velocity over time, such that HM ∈ [0, 10] dB and TTT ∈ [0, 5.12] s. Thus, the system individually deals with each user so that the SON algorithm determines the appropriate HM and TTT values.
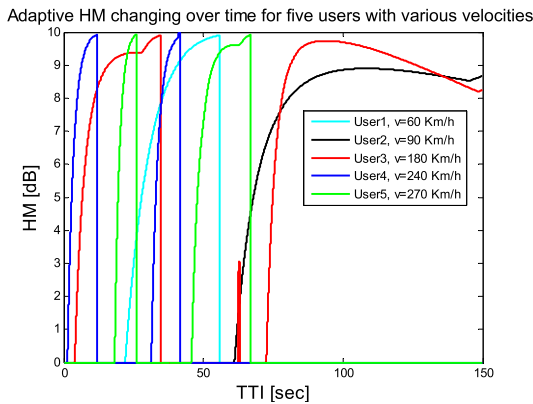
FIGURE 22. Illustrating how the adaptive HM changing over time and velocity for five users having different speed, for the scenario 6, X = 1000, N = 91, ST = 150 [s], T_{crit} = 2 [s].
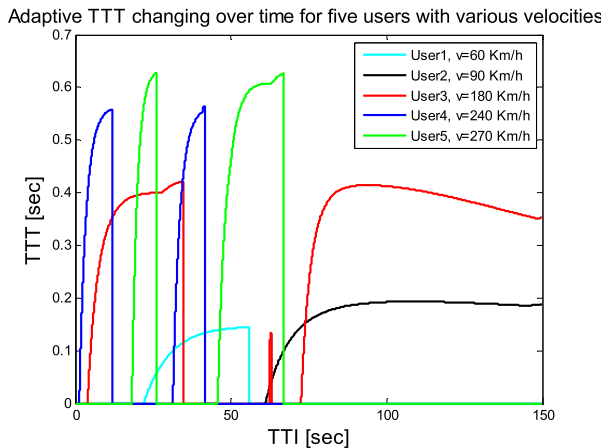
FIGURE 23. Illustrating how the adaptive TTT changing over time and velocity for five users having different speed, for the scenario 6, X = 1000, N = 91, ST = 150 [s], T_{crit} = 2 [s].

VII. MORE RESULTS: DISCUSSION, ACCURACY AND VALIDITY

In this section, we use the simulation results of the fifth scenario (X = 3000 users, N = 91 small cells, ST = 150 s,
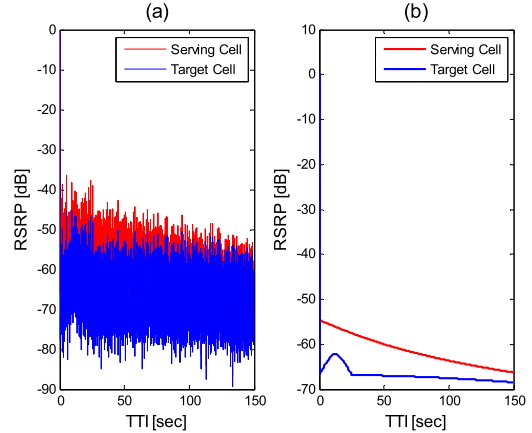

FIGURE 24. Illustrating the RSRP of the serving and target cells, for an arbitrary UE moving with velocity of 30 km/h, (a) with shadowing fading and (b) the average RSRPs.

T_{crit} = 6 s) to discuss some important issues related to the accuracy and validity of our model. Let us first consider an arbitrary user served by a macro cell and move with a velocity of 30 km/h, taking into account its initial location in the network. Fig. 24 illustrates the RSRP of both the target and the serving cell of this UE. We notice from this figure that $RSRP_i^{serving}(t) > RSRP_i^{target}(t)$ is always satisfied, where Fig. 24-(a) corresponds to considering the shadow fading gain added according to the Equation (3), while Fig. 24-(b) represents the average RSRPs. As we found from the simulation, both $HM_{adaptive}$ and $TTT_{adaptive}$ remain zero during the entire UE's mobility, which is consistent with the explanation listed at the end of the two subsections V.1 and V.2. Hence, for 150 s, this UE will still be served by the same microcell, although this UE moves throughout dense small cells, and the idiosyncratic pair (HM = 0, TTT = 0) is the most suitable one for this UE as long as the RSRP of the serving cell is always larger than that of the target cell, that is, there is no need to make any HO decision.
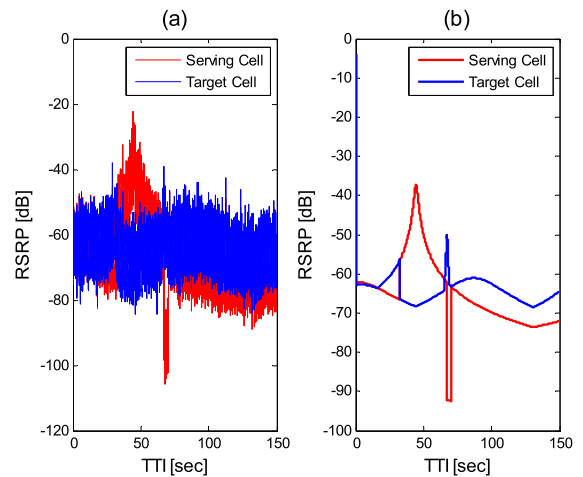

FIGURE 25. Illustrating the RSRP of the serving and target cells, for another UE moving with velocity of 30 km/h, (a) with shadowing fading and (b) the average RSRPs.
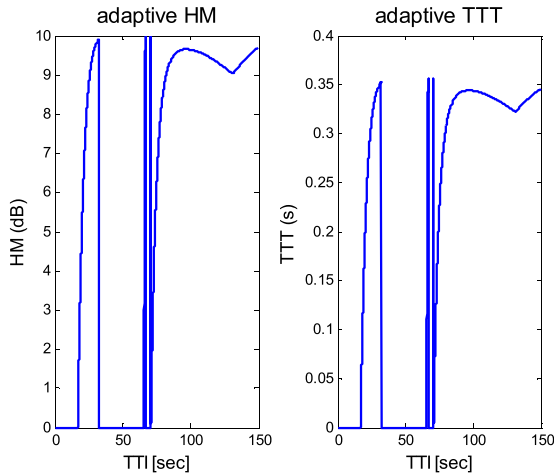
FIGURE 26. Illustrating the adaptive HM and TTT, for the second UE moving with velocity of 30 km/h.

FIGURE 27. Illustrating the serving sequence for the second UE moving with velocity of 30 km/h.

FIGURE 28. Illustrating the RSRP of the serving and target cells, for the third UE moving with velocity of 90 km/h, (a) with shadowing fading and (b) the average RSRPs.

Let us now consider another UE moving at 30 km/h with a deferent initial location. Fig. 25 illustrates the RSRPs of both the target and serving cell, similar to Fig. 24, but with different situations. For this UE, we found that both HM$_{adaptive}$ (ranges from 0 to 10 dB) and TTT$_{adaptive}$ (ranging from 0 to 350 ms) take different positive values during mobility, as shown in Fig. 26. In our simulation, we considered that the macrocells were numbered from 901 to 919 (19 cells), while the small cells were numbered from 1001 to 1091 (91 small cells). Fig. 27 illustrates the serving sequence of the UE considered in the second example. We notice from Fig. 27 that there is three HO decisions made for this UE, the first is such that the UE is handed over from the small cell numbered 1018 to the macro cell numbered 909 at the moment $t = 32.64$ s, and then it is handed over from the macro cell numbered 909 to the small cell numbered 1083 at the moment $t = 67.24$ s and then, in a period of time equals to 3.16 s, that is less than the critical ping-pong time $T_{criti} = 6$ s, the UE is handed over back to the macro cell numbered 909 at the moment t = 70.4 s, which means that a ping-pong event has occurred between the moments 67.24 s and 70.4 s. We found that the first HO decision was successful without the occurrence of an RLF event (neither TLHO nor TEHO), but both the second and third HO decisions introduced a UHO (a ping-pong event). This is a clear example that our model does not completely eliminate ping-pong events, but it can easily reduce their number as much as possible using the idiosyncratic adaptive model for HM and TTT, providing much lower HPI$_{PPHOR}$ than the literature as we have seen in the previous section.

Let us now consider a third user moving with 90 km/h again with an initial location different from those of the previous two users. Fig. 28 illustrates the RSRPs of both target and serving cell of this user. For this user, we found that both HM$_{adaptive}$ (ranging from 0 to 10 dB) and TTT$_{adaptive}$ (ranging from 0 to 214 ms) take different positive values during mobility, as shown in Fig. 29.
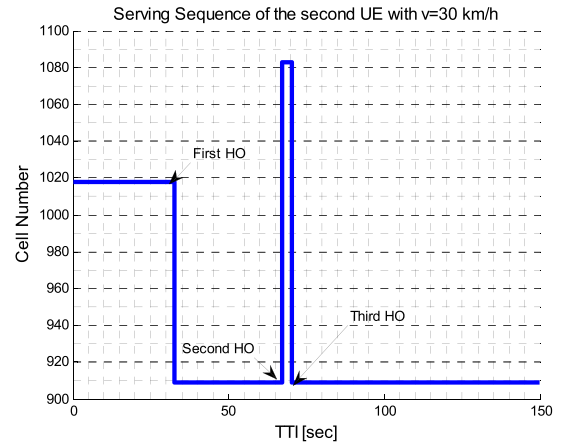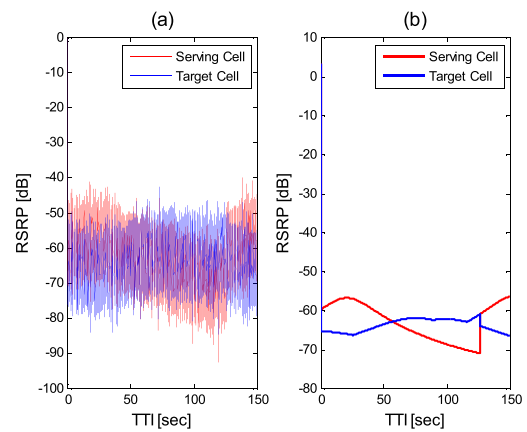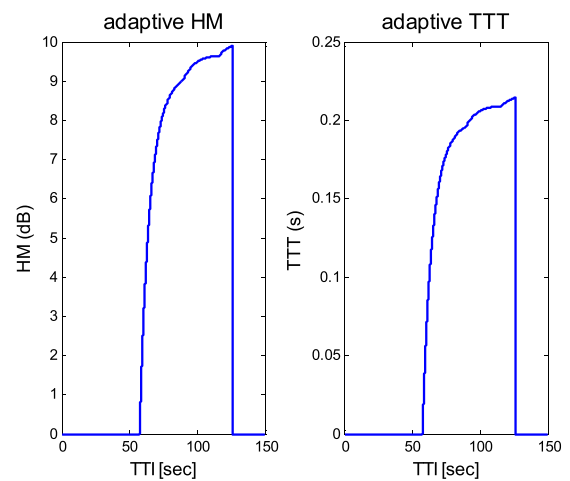

FIGURE 29. Illustrating the adaptive HM and TTT, for the third UE moving with velocity of 90 km/h.

The accuracy of our model is shown in the third example. From Fig. 28, we notice that there is a clear case in which the RSRP of the target cell is greater than that of the serving cell

in the time range from 50 to 100 s during the movement of this user, and HM values were calculated as shown in Fig. 29. However, our algorithm did not decide to send an HRQ until after $t = 100$ s. The simulation indicates that, for this user, if HRQ had been sent (between 50 and 100 s) there would have been a TLHO or TEHO event. Thus, Equation (11) has chosen values for HM that are suitable for the HO decision where the SINR is relatively strong for both the current serving cell and the target serving cell (each one of the inequalities of SINR is larger than Θ). In addition, according to the velocity value of the UE, Equation (14) returns a suitable value for TTT that should force inequality (10) to be held at the right moment. Otherwise, it would lead to a service interruption due to TEHO or TLHO. Here, it is the meaning of the "suitable adaptive" values of both HM and TTT, that is, it is to prevent HRQ from being sent at the wrong moment. Therefore, we say here that the pair (HM$_{adaptive}$, TTT$_{adaptive}$) is idiosyncratic for this third UE such that the wrong HO decision is prevented indirectly. The successful HO decision is made after 100 s for this third user (actually at the moment $t = 126$ s), where the target cell took the role of the serving cell, that is, its color changed from blue to red according to the color representation adopted in our simulations. Fig. 30 illustrates the serving sequence of the third UE ensuring that there is no HRQ between 50 and 100 s, while this UE is handed over from the small cell numbered 1001 to the macro cell numbered 915 at the moment $t = 126$ s, again without RLF HO events.
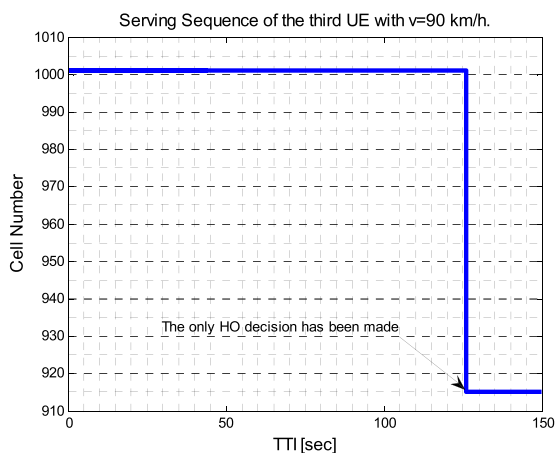

FIGURE 30. Illustrating the serving sequence for the third UE moving with velocity of 90 km/h.

In general, it has been reported in the literature that setting high values of HM and TTT at high speeds will cause a higher rate of HOF when a user moves at high speeds. However, there is still no standard definition about the meaning of "bad high", "good high", "bad small", or "good small" values of HM and TTT regarding to the PPHO and HOF issues. In addition, there is no standard definition of speed limits corresponding to each of these meanings. In fact, the RSRP represents a random quantity in the communication mobile systems owing to the randomness of the fading phenomena of

the communication channel; hence, both the RLF HO event (TLHO or TEHO) and PPHO event are random events in the first place. In this regard, one of the main ideas that brought us to our model is that we consider that talking about "high values" or "small values" of HM, TTT and UE's velocity should be relative and adaptive to the state of the user's mobility and to the state of cell positions in the network (geographical positions, i.e., cell positions and its distances to the user and hence the relative values of the RSRP and the SINR). The fourth example confirms this view according to the results of our proposed model. We show now that the general idea that says "*high values of HM and TTT during high speed will cause higher rate of HOF when a user moves in high speeds*" is not always true. Fig. 31 shows the servicing sequence for a user (from Scenario 5) moving at a velocity of 240 km/h ("very high" speed), where the UE is handed over from the small cell numbered 1007 to the macro cell numbered 915.
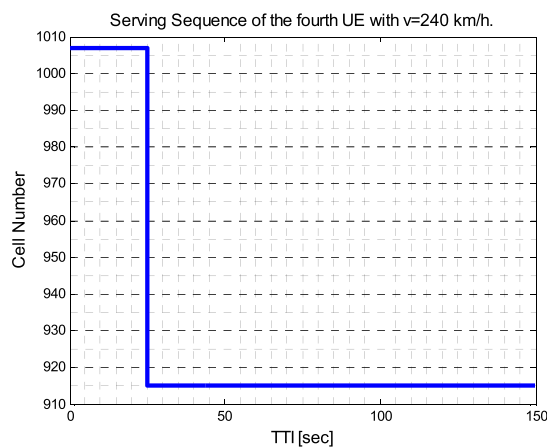

FIGURE 31. Illustrating the serving sequence for the fourth UE moving with velocity of 240 km/h.

Fig. 32 shows the RSRP curves of both serving and target cells of the fourth user, and expresses the state of the user sites in relation to both the serving cell and the target cell. We notice from Fig. 32 that the values of RSRP of the target cell are greater than those of the current serving cell just before the HO decision is made, and this means that the third inequality in the Equation (11) has been achieved before making the HO decision.

Fig. 33 shows the average SINR curves of the serving cell and the target cell. we notice from Fig. 33 that the SINR values for both the target cell and the serving cell also achieve the first and second conditional inequalities of the Equation (11), where both of them are on average greater than the system threshold ($\Theta = -35$ dB) in each time window of length $W = 200$ ms prior until reaching to the moment of the HO decision. We notice here that the HO decision was made here at the moment when the red and blue colors of the curves were swapped (which means a state of transit, i.e., service transition from the current serving cell to the target cell, knowing that each curve of either serving or target
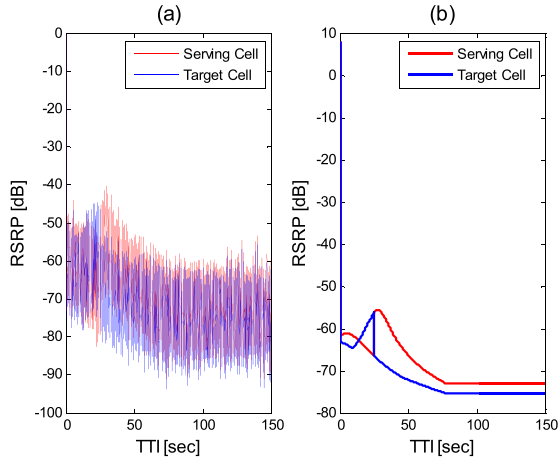
FIGURE 32. Illustrating the RSRP of the serving and target cells, for the fourth UE moving with velocity of 240 km/h, (a) with shadowing fading and (b) the average RSRPs.
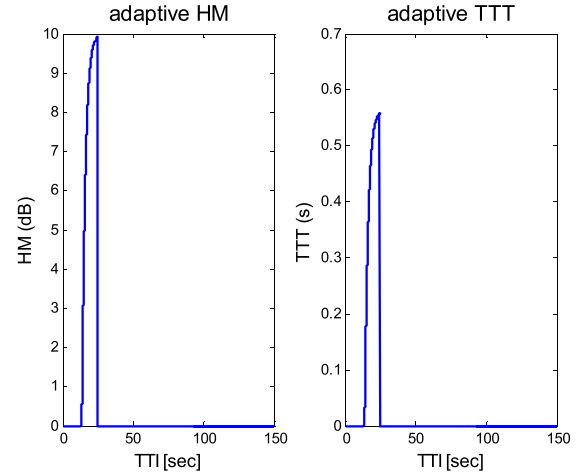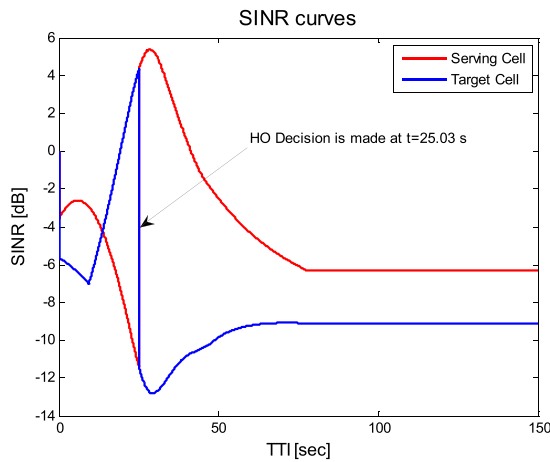

FIGURE 33. Illustrating the average SINR of the serving and target cells, for the fourth UE moving with velocity of 240 km/h.

FIGURE 34. Illustrating the adaptive HM and TTT, for the fourth UE moving with velocity of 240 km/h.
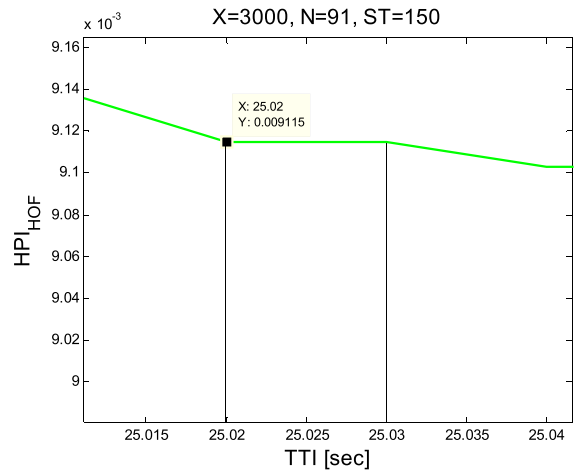

FIGURE 35. Illustrating that the HPI$_{HOF}$ of the scenario 5 remains constant between the two moments 25.02 and 25.03.

cell has two colors, red and blue to distinguishing between before and after the HO decision is made, as we did in Fig. 6).

Fig. 34 shows the values of each of HM adapted according to Equation 11 and the values of TTT adapted to the values of HM and the "very high" speed of this user according to the Equation (14), where the highest TTT value is 558 ms corresponding to the moment of time when the HO decision is made for this UE whose velocity equals 240 km/h. Note here that the value of TTT in Table 1 corresponding to the high speed of 230 km/h is 5120 ms, but the Equation (14) return 558 ms. In fact, it is not Table 1 what we use to select the adaptive TTT, but the main aim of constructing Table 1 is only to develop a proper TTT adaptive function in terms of both adaptive HM and velocity, and this function is only expressed by the Equation (14) and Fig. 8.

As the main result, and by zooming in Fig. 19, Fig. 35 confirms that the HPI$_{HOF}$ of our algorithm remains constant between the moments 25.02 s and 25.03 s, which means that there is no HOF event corresponding to this period of

time, which confirms that the combination of relatively high adaptive value of TTT with adaptive HM and high velocity does not necessarily lead, according to our model, to an RLF HO event.

This example shows that the "relative high velocity" along with "high relative values of HM and TTT" do not necessarily lead to RLF problems, as we have an HO here but without an RLF HO event. That is, having high relative values of HM, TTT, and velocity that do not necessarily lead to an RLF event. Thus, it can be said that the value of the corresponding TTT is not "so high" in this case, and it is even not "very high" following the traditional view on the adjective "high" for TTT value since the high values of the TTT according to the basic 3GPP are those that are more than 1024 ms, but we obtained a value less than 560 ms. This is although the velocity is high (240 km/h). This means that our model is able to match this user state to the network and produce appropriate values for both HM and TTT so that we have a valid successful HO decision.

Our proposed model presents a mechanism for choosing the values of both HM and TTT adaptively according to RSRP, SINR, and the user's velocity without classifying the velocity values into predefined groups. We developed Equations (11) and (14) so that they look at the system holistically. This means that they are suitable for any velocity within the range considered in the manuscript. In this study, we introduce the approach of selecting HM and TTT so that it can be valid for any mobile communication scenario with regard to the HO decision issue; and the most important recommendation that can be obtained here is the need to think about the existence of a relationship between HM and TTT and study it in some scenarios. To the best of our knowledge, this has not been previously discussed, in the literature, regarding the possibility of such a relationship, or about its investment in developing a mechanism for selecting the values of HM and TTT. Therefore, our study can be considered a starting point in this direction. In this context, we encourage readers to apply our proposed model to other scenarios in terms of changing the type of network, for example, LTE-R, or in terms of the pattern and nature of user mobility, for example, high-speed railway scenarios. At the same time, we recommend thinking about the HCPs (HM, TTT) in another way, in the sense of looking for other formulas for the relationship between them, which can be more accurate or comprehensive than Equations (11) and (14).

Regarding the PPHO indicator results, the ping-pong indicator defined in Subsection III.D.2 does not increase absolutely over time. First of all, let's focus on all the figures related to this indicator in Section VI, then one can obviously notice that the trend of variation of each those curves locally changes from time to time. This is true not only for the curves corresponding to our proposed algorithm's performance, but also for each curve of the other literature (as in [9]), we compare with. For example, as shown in Fig. 20, in the time range from 50 to 100 s, where the HPIHOPP tends to decrease for some moments, to increase for some other, or to be constant for some other moments. We can also observe this in Fig. 10. In addition, as shown in Fig.18, after a specific time has passed, some curves tend to be almost constant, on average, with the passage of time. We also notice this in Figure 16. However, one may expect that the general changes of curves tend to be continually increasing, but this is only partially true if two separate moments are considered, that is, by taking two specific points from each curve, so that these two points are very special. In this regard, we should emphasize here that the mobility model that we impose on users moving in a network environment plays an important role in obtaining PPHO events. Returning to Subsection III.B, one can notice that we impose on users to return to the network environment in the event of exceeding the geographical boundaries of this network. Therefore, the number of PPHO events can relatively increase, because the user may return to the same area from which he exited; thus, the same PPHO event will be repeated again. Herein lies the power of our model in selecting the adaptive values for HM and TTT considering

this worse case of mobility. Compared with Fig. 3-5, 3-6, 3-7 of [9], one can clearly notice the similarity of change tendency of PPHO with [9]. We should add here that the literature we are compared with has adopted simulation method so that the same speed is assigned to all simulated users to calculate the number of PPHOs; however, the PPHOR figures are obtained in this study so that all users move, during the simulation run, at different speeds within the network. Herein lies the power of our simulation approach.

VIII. FUTURE IMPROVEMENT

As a future plan, we could include further KPIs, such as throughput, call drop rate (CDR), long interruption time (IT), and HO delay, along with new applications of our proposed algorithm in the fifth generation (5G) HetNets. We could also consider a multi-tier (i.e., three or four tiers) HetNets scenario including not only femto BSs, but also micro and pico BSs. In this regard, we can compare the performance of our model with the conditional HO models proposed for 5G HetNets. However, HO parameter self-optimization is still an up-to-date significant function that will be introduced in 5G and even in the sixth generation (6G) mobile networks. The automatic self-optimization operation characteristics would enable this adaptation to be part of the next mobile generation with further improvements. Several SON algorithms have been proposed to optimize HCPs automatically under different scenarios. However, no study has investigated the relationship between HCPs. From this standpoint, our proposed solution appears to be a promising starting point in this regard, by mathematically developing its main adaptive equations with a general analytical approach, and utilizing various simulation environments and scenarios to determine which models perform better. The number of mobile communications will increase significantly in the near future. This results in an increasing number of ultra-dense networks in terms of small cells. This results in a significant increase in the need for load balancing. This requires further self-optimization to balance the load between the cells. There are a plenty of work that deal with adjusting both of the handover parameters according to the status of the network load, e.g., [52]. However, as we mentioned before, the new knowledge that our paper presents here is reflected in the study of a possible relationship between the HCPs so that it can be invested in adaptively selecting HM and TTT according to the status of the network. The work in [52] deals with the problem of adjusting the HCPs such that the HM takes specific unjustified values in accordance with a non-general classification of the UE velocity regarding only the macro cell load (as shown in Table 2 of [52]) without considering the small cell load case. This leads us to a possible improvement in combining our solution with [52] by using our adaptive technique directly in selecting the proper HM values. In fact, the authors of [52] used only three categories of HM values that were very small, which led to a large number of UHOs in HetNet. In other words, [52] proposed an adjusting technique only in the sense of the cell load without any processing to

other system requirements with regard to KPIs. Moreover, Table 3 of [52] again uses specific fixed and large TTT values assumed for the three insufficient velocity categories, which implies a large probability of increasing TEHO and TLHO events. As a result, our work can be combined with [52] as a future improvement in this field. This is in the sense of directly evaluating our algorithm by incorporating the proposed HO decision model into the study of the load-balancing issue in HetNets.

IX. CONCLUSION

In this work, we presented a completely adaptive mechanism to setup the HCPs with regard to making HO decisions within HetNet, considering the user's mobility state. This novel mechanism was formulated in the context of the SON algorithm to support the MRO in LTE-A networks in response to system requirements. The algorithm proposed here aimed to reduce the number of PPHOs and RLF HOs to almost zero. This new algorithm selects HCPs adaptively to both the user's location and velocity. This is achieved by developing innovative functions that rely on basic HO decision parameters, such as the RSRP and SINR. Hence, a robust relationship between HM, TTT, and UE velocity was discovered. This was done without the need for any predefined HOFR or PPHOR thresholds or the need for unjustified steps for tuning the HCPs. Our study showed that HCPs are correlated with each other. This correlation is an urgent need to determine the proper HCP values to make a proper HO decision considering UE mobility. Thus, this correlation could become necessary as a basic requirement of any future SON algorithm considering the existence of a functional relationship between HM and TTT, such that they should not be set in isolation from each other, as in the literature. As a basic result, we say that resetting HCPs to meet the requirements of user mobility must, in some way, assume a direct relationship between these parameters and not be considered as independent parameters at the system level. This consideration clearly raises the performance of the system in general, as we have seen in the Results section, and undoubtedly supports the need to consider such a relationship between HM and TTT with regard to MRO.

APPENDIX

Using Microsoft Excel©, we present here the derivation steps of Equation (14) (the same steps are used for Equation (15)):

Step1: Importing **TTT** data and $\frac{1}{\mathbf{v} \times \mathbf{HM}_{\mathbf{adaptive}}}$ of Table 1 into an Excel worksheet, as shown in Fig. 36.

Step 2: Inserting a scatter plot for the above Excel data, as illustrated in Fig. 37. Thus, we obtain figures 8 and 9.

Step 3: Add a trendline plot of type "Power" and check the corresponding box to show the resultant equation, as shown in Fig. 38.

The power trend line is very similar to the exponential curve; it has a more symmetrical arc. It is commonly used to plot measurements that increase at a certain rate. The trend

TABLE 9. List of abbreviations in A-to-Z order.

| Description	Item
3rd Generation Partnership Project	3GPP
Base Station	BS
Call Drop Rate	CDR
evolved Node BS	eNB
Fifth Generation	5G
First Generation	1G
Fuzzy Logic Controller	FLC
Global Positioning System	GPS
Handover	HO
Handover Failure Ratio	HOFR
Heterogeneous Networks	HetNets
HO Control Parameters	HCPs
Hysteresis Margin	HM
HO Request	HRQ
Home eNB	HeNB
Interruption Time	IT
Key Performance Indicators	KPI
Long-Term Evolution-Advanced	LTE-A
Macro eNB	MeNB
Mobility Robustness Optimization	MRO
Ping Pong Handover	PPHO
Ping Pong Handover Ratio	PPHOR
Quality of Service	QoS
Radio Link Failure	RLF
Reference Signal Received Power	RSRP
Received-Signal-Strength	RSS
Radio Resource Control	RRC
Self-Optimization Networks	SON
Signal-to-Interference-plus-Noise-Ratio	SINR
Sixth Generation	6G
Small eNB	SeNB
Time-To-Trigger	TTT
Too-Early HO	TEHO
Too-Late HO	TLHO
Transmission Time Interval	TTI
Unnecessary HO	UHO
User Equipment	UE
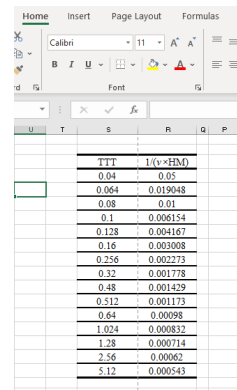
FIGURE 36. Importing TTT and 1/(v × HM) data into Excel worksheet.

lines method is a common mathematical method used in the sense of nonlinear regression concept, aiming to find a
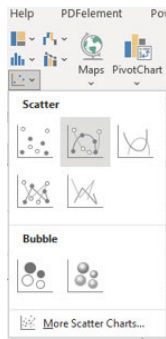
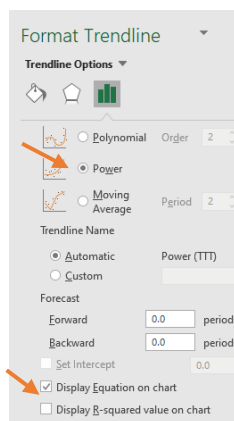**FIGURE 37. Inserting a scatter plot for TTT and 1/(v × HM) data.**

FIGURE 38. Inserting a scatter plot for TTT and 1/(v × HM) data.

suitable curve of a function fitting a sample of data and to estimate the corresponding equation.

ACKNOWLEDGMENT

REFERENCES

[1] Cisco, "Cisco visual networking index: Global mobile data traffic forecast update, 2014–2019," Cisco, San Jose, CA, USA, White paper FLGD 12083, Feb. 2015.

[2] O. O. Omitola and V. M. Srivastava, "A robust speed-based handover algorithm for dense femtocell/macrocell LTE—A network and beyond," *J. Telecommun., Electron. Comput. Eng.*, vol. 8, no. 9, pp. 121–129, Dec. 2016.

[3] T. Zahir, K. Arshad, A. Nakata, and K. Moessner, "Interference management in femtocells," *IEEE Commun. Surveys Tuts.*, vol. 15, no. 1, pp. 293–311, 1st Quart., 2013.

[4] P. Munoz, R. Barco, and I. D. L. Bandera, "On the potential of handover parameter optimization for self-organizing networks," *IEEE Trans. Veh. Technol.*, vol. 62, no. 5, pp. 1895–1905, Jun. 2013.

[5] Q. Liao, F. Penna, S. Stanczak, Z. Ren, and P. Fertl, "Context-aware handover optimization for relay-aided vehicular terminals," in *Proc. IEEE 14th Workshop Signal Process. Adv. Wireless Commun. (SPAWC)*, Jun. 2013, pp. 555–559.

[6] T. Jansen, I. Balan, J. Turk, I. Moerman, and T. Kurner, "Handover parameter optimization in LTE self-organizing networks," in *Proc. IEEE 72nd Veh. Technol. Conf. (Fall)*, Sep. 2010, pp. 1–5.

[7] *Radio Resource Control (RRC); Protocol Specification*, document TS 36.331, 3GPP, Version 15.3.0, Release 15, France, 2018. [Online]. Available: https://www.etsi.org/deliver/etsi_ts/136300_136399/136331/15.03.00_60/ts_136331v150300p.pdf

[8] C.-H. Chen, C.-A. Lee, and C.-C. Lo, "Vehicle localization and velocity estimation based on mobile phone sensing," *IEEE Access*, vol. 4, pp. 803–817, 2016.

[9] B. Zhang, "Handover control parameters optimization in LTE networks," Ph.D. dissertation, Dept. Elect. Eng., Univ. Sheffield, Sheffield, U.K., Apr. 2018.

[10] A. Ulvan, R. Bestak, and M. Ulvan, "The study of handover procedure in LTE-based femtocell network," in *Proc. WMNC*, Oct. 2010, pp. 1–6.

[11] A. Ulvan, R. Bestak, and M. Ulvan, "Handover procedure and decision strategy in LTE-based femtocell network," *Telecommun. Syst.*, vol. 52, no. 4, pp. 2733–2748, Apr. 2013.

[12] H. Zhang, W. Ma, W. Li, W. Zheng, X. Wen, and C. Jiang, "Signalling cost evaluation of handover management schemes in LTE-advanced femtocell," in *Proc. IEEE 73rd Veh. Technol. Conf. (VTC Spring)*, May 2011, pp. 1–5.

[13] S.-J. Wu, "Handover strategy in HIP-based LTE femtocells networks with hybrid access mode," in *Proc. 6th Int. Conf. Genetic Evol. Comput.*, Aug. 2012, pp. 571–576.

[14] R. D. Hegazy and O. A. Nasr, "A user behavior based handover optimization algorithm for LTE networks," in *Proc. IEEE Wireless Commun. Netw. Conf. (WCNC)*, Mar. 2015, pp. 1255–1260.

[15] M. Alhabo and L. Zhang, "Unnecessary handover minimization in two-tier heterogeneous networks," in *Proc. 13rd Annu. Conf. Wireless Demand Netw. Syst. Services (WONS)*, Feb. 2017, pp. 160–164.

[16] A. Kishida, Y. Morihiro, T. Asai, and Y. Okumura, "Cell selection scheme for handover reduction based on moving direction and velocity of UEs for 5G multi-layered radio access networks," in *Proc. Int. Conf. Inf. Netw. (ICOIN)*, Jan. 2018, pp. 362–367.

[17] S. Kapoor, D. Grace, and T. Clarke, "A base station selection scheme for handover in a mobility-aware ultra-dense small cell urban vehicular environment," in *Proc. IEEE 28th Annu. Int. Symp. Pers., Indoor, Mobile Radio Commun. (PIMRC)*, Oct. 2017, pp. 1–5.

[18] J.-M. Moon and D.-H. Cho, "Efficient handoff algorithm for inbound mobility in hierarchical macro/femto cell networks," *IEEE Commun. Lett.*, vol. 13, no. 10, pp. 755–757, Oct. 2009.

[19] J. Moon and D. Cho, "Novel handoff decision algorithm in hierarchical macro/femto-cell networks," in *Proc. IEEE Wireless Commun. Netw. Conf.*, Apr. 2010, pp. 1–6.

[20] K. Alexandris, N. Sapountzis, N. Nikaein, and T. Spyropoulos, "Load-aware handover decision algorithm in next-generation HetNets," in *Proc. IEEE Wireless Commun. Netw. Conf.*, Apr. 2016, pp. 1–6.

[21] P. Xu, X. Fang, R. He, and Z. Xiang, "An efficient handoff algorithm based on received signal strength and wireless transmission loss in hierarchical cell networks," *Telecommun. Syst.*, vol. 52, no. 1, pp. 317–325, Jan. 2013.

[22] D. Lopez-Perez, A. Ladanyi, A. Juttner, and J. Zhang, "OFDMA femto-cells: Intracell handover for interference and handover mitigation in two-tier networks," in *Proc. IEEE Wireless Commun. Netw. Conf.*, Apr. 2010, pp. 1–6.

[23] D. López-Pérez, A. Valcarce, Á. Ladányi, G. de la Roche, and J. Zhang, "Intracell handover for interference and handover mitigation in OFDMA two-tier macrocell-femtocell networks," *EURASIP J. Wireless Commun. Netw.*, vol. 2010, no. 1, Feb. 2010, Art. no. 142629.

[24] H. Kalbkhani, S. Yousefi, and M. G. Shayesteh, "Adaptive handover algorithm in heterogeneous femtocellular networks based on received signal strength and signal-to-interference-plus-noise ratio prediction," *IET Commun.*, vol. 8, no. 17, pp. 3061–3071, Nov. 2014.

[25] T. Jansen, I. Balan, S. Stefanski, I. Moerman, and T. Kurner, "Weighted performance based handover parameter optimization in LTE," in *Proc. IEEE 73rd Veh. Technol. Conf. (VTC Spring)*, May 2011, pp. 1–5.

[26] M. S. I. Khan, M. M. Rahman, K. Raahemifar, J. Mišić, and V. B. Mišić, "Self-optimizing control parameters for minimizing ping-pong handover in long term evolution (LTE)," in *Proc. 27th Biennial Symp. Commun. (QBSC)*, Jun. 2014, pp. 118–122.

[27] N. Hassan, K. Elkhazeen, K. Raahemifar, and X. Fernando, "Optimization of control parameters using averaging of handover indicator and received power for minimizing ping-pong handover in LTE," in *Proc. IEEE 28th Can. Conf. Electr. Comput. Eng. (CCECE)*, May 2015, pp. 92–97.

[28] D.-W. Lee, G.-T. Gil, and D.-H. Kim, "A cost-based adaptive handover hysteresis scheme to minimize the handover failure rate in 3GPP LTE system," *EURASIP J. Wireless Commun. Netw.*, vol. 2010, no. 1, Dec. 2010, Art. no. 750173.

[29] P. Xu, X. Fang, J. Yang, and Y. Cui, "A user's state and SINR-based handoff algorithm in hierarchical cell networks," in *Proc. Int. Conf. Comput. Intell. Softw. Eng.*, Sep. 2010, pp. 1–4.

[30] M. Vondra and Z. Becvar, "Connection cost based handover decision for offloading macrocells by femtocells," in *Proc. Int. Conf. Wired/Wireless Internet Commun.*, 2012, pp. 208–219.

[31] Z. Becvar and P. Mach, "Adaptive hysteresis margin for handover in femtocell networks," in *Proc. 6th Int. Conf. Wireless Mobile Commun.*, Sep. 2010, pp. 256–261.

[32] S. Lal and D. K. Panwar, "Coverage analysis of handoff algorithm with adaptive hysteresis margin," in *Proc. 10th Int. Conf. Inf. Technol. (ICIT)*, Dec. 2007, pp. 133–138.

[33] M. Boujelben, S. Ben Rejeb, and S. Tabbane, "A novel green handover self-optimization algorithm for LTE—A/5G HetNets," in *Proc. Int. Wireless Commun. Mobile Comput. Conf. (IWCMC)*, Aug. 2015, pp. 413–418.

[34] G. Araniti, J. Cosmas, A. Iera, A. Molinaro, A. Orsino, and P. Scopelliti, "Energy efficient handover algorithm for green radio networks," in *Proc. IEEE Int. Symp. Broadband Multimedia Syst. Broadcast.*, Jun. 2014, pp. 1–6.

[35] G. Yang, X. Wang, and X. Chen, "Handover control for LTE femtocell networks," in *Proc. Int. Conf. Electron., Commun. Control (ICECC)*, Sep. 2011, pp. 2670–2673.

[36] M. Z. Chowdhury, W. Ryu, E. Rhee, and Y. M. Jang, "Handover between macrocell and femtocell for UMTS based networks," in *Proc. 11st Int. Conf. Adv. Commun. Technol.*, Feb. 2009, pp. 237–241.

[37] M. Alhabo, L. Zhang, and O. Oguejiofor, "Inbound handover interference-based margin for load balancing in heterogeneous networks," in *Proc. Int. Symp. Wireless Commun. Syst. (ISWCS)*, Aug. 2017, pp. 146–151.

[38] D. Xenakis, N. Passas, L. Merakos, and C. Verikoukis, "Energy-efficient and interference-aware handover decision for the LTE-advanced femtocell network," in *Proc. IEEE Int. Conf. Commun. (ICC)*, Jun. 2013, pp. 2464–2468.

[39] H. Zhang, C. Jiang, and J. Cheng, "Cooperative interference mitigation and handover management for heterogeneous cloud small cell networks," *IEEE Wireless Commun.*, vol. 22, no. 3, pp. 92–99, Jun. 2015.

[40] A. D. Antoro, I. W. Mustika, and S. B. Wibowo, "Downlink cross-tier interference mitigation for macrocell user in open access femtocell using handover scenario," in *Proc. Int. Conf. Electr. Eng. Informat. (ICEEI)*, Aug. 2015, pp. 656–660.

[41] I. Shayea, M. Ergen, A. Azizan, M. Ismail, and Y. I. Daradkeh, "Individualistic dynamic handover parameter self-optimization algorithm for 5G networks based on automatic weight function," *IEEE Access*, vol. 8, pp. 214392–214412, 2020.

[42] A. Alhammadi, M. Roslee, M. Y. Alias, I. Shayea, and A. Alquhali, "Velocity-aware handover self-optimization management for next generation networks," *Appl. Sci.*, vol. 10, no. 4, p. 1354, Feb. 2020.

[43] A. Abdulraqeb, R. Mardeni, A. M. Yusoff, S. Ibraheem, and A. Saddam, "Self-optimization of handover control parameters for mobility management in 4G/5G heterogeneous networks," *Autom. Control Comput. Sci.*, vol. 53, no. 5, pp. 441–451, Nov. 2019.

[44] K. Da Costa Silva, Z. Becvar, and C. R. L. Frances, "Adaptive hysteresis margin based on fuzzy logic for handover in mobile networks with dense small cells," *IEEE Access*, vol. 6, pp. 17178–17189, 2018.

[45] M Series, "Guidelines for evaluation of radio interface technologies for IMT-2020," ITU, Geneva, Switzerland, Tech. Rep. ITU-R M. 2412-0, 2017. [Online]. Available: https://www.itu.int/md/R15-SG05-C-0057

[46] (2021). *SINR Map for a 5G Urban Macro-Cell Test Environment-MATLAB & Simulink*. [Online]. Available: https://www.mathworks.com/help/phased/ug/sinr-map-for-a-5g-urban-micro-cell-test-environment.html

[47] L. F. Ibrahim, H. A. Salman, Z. F. Taha, N. Akkari, G. Aldabbagh, and O. Bamasak, "A survey on heterogeneous mobile networks planning in indoor dense areas," *Pers. Ubiquitous Comput.*, vol. 24, no. 4, pp. 487–498, Aug. 2020.

[48] A. Alhammadi, M. Roslee, M. Y. Alias, I. Shayea, S. Alraih, and K. S. Mohamed, "Auto tuning self-optimization algorithm for mobility management in LTE—A and 5G HetNets," *IEEE Access*, vol. 8, pp. 294–304, 2020.

[49] P.-C. Lin, L. F. G. Casanova, and B. K. S. Fatty, "Data-driven handover optimization in next generation mobile communication networks," *Mobile Inf. Syst.*, vol. 2016, p. 11, Aug. 2016.

[50] *LTE; Evolved Universal Terrestrial Radio Access (E-UTRA); Requirements for Support of Radio Resource Management*, document TS 36.133, 3GPP, Version 15.8.0, Release 15, 2019.

[51] Y. Li, B. Cao, and C. Wang, "Handover schemes in heterogeneous LTE networks: Challenges and opportunities," *IEEE Wireless Commun.*, vol. 23, no. 2, pp. 112–117, Apr. 2016.

[52] M. Alhabo and L. Zhang, "Load-dependent handover margin for throughput enhancement and load balancing in HetNets," *IEEE Access*, vol. 6, pp. 67718–67731, 2018.

[53] M. Behjati and J. Cosmas, "Multi-layer cell deployment strategy for self-organizing LTE-advanced networks," in *Proc. 9th Int. Wireless Commun. Mobile Comput. Conf. (IWCMC)*, Jul. 2013, pp. 820–825.

[54] *LTE; Evolved Universal Terrestrial Radio Access (E-UTRA); User Equipment (UE) Conformance Specification Radio Transmission and Reception; Part1: Conformance Testing*, document TS 36.521-1, 3GPP, Version 8.3.1 Release 8, 2009.

TAREK AL ACHHAB was born in Damascus, Syria, in 1987. He received the B.S. degree in electronic and telecommunication engineering and the M.S. degree in advanced telecommunication engineering from Damascus University, in 2009 and 2016, respectively, where he is currently pursuing the Ph.D. degree.

He has more than ten years of professional experience in optical transmission networks and FTTX networks (planning, implementation, and configuration) at Syrian Telecom Company, from 2010 to 2021. Currently, he is teaching at the Electronics and Communication Engineering Department, Damascus University. His research interests include WiMAX network planning and automatic neighbor relation (ANR) in LTE self-optimization network (SON) and performance optimization of wireless communication systems.

FARIZ ABBOUD received the B.S. degree in electronic engineering from Damascus University, Damascus, Syria, in 1979, and the M.S. degree in astrophysics and the Ph.D. degree in microstrip antenna from the University of Nice Sophia Antipolis, Nice, France, in 1985 and 1988, respectively.

In 1990, he worked as the Project Manager at HPF Company (CT2 project), La Haute, Annecy, France. Since 2005, he has been a Professor with the Electronic and Telecommunication Department, Damascus University. He is the author of four books and more than 100 articles. His research interests include microstrip antennas, microwave filters, acoustics, and wireless communication systems. He was a Reviewer of IEEE TRANSACTIONS ON ANTENNAS AND PROPAGATION, in 1989.

ABDULKARIM ASSALEM received the B.S. degree in electronic engineering from Damascus University, Damascus, Syria, in 1984, and the M.S. degree in antenna and microwaves and the Ph.D. degree in collimator for antenna measurements in near zone field from the Communications Institute, Russia, in 1988 and 1992, respectively.

From 1992 to 1998, he was a Research Assistant and a Lecturer at Al-Baath University, Homs, Syria. He was also the Head of the Electronic and Communication Department, Al-Baath University, where he has been a Professor with the Electronic and Telecommunication Department, since 2005. He is the author of eight books and more than 45 articles. His research interests include antennas, microwaves, optical networks, and wireless communication systems.